Hindawi
Journal of Advanced Transportation
Volume 2020, Article ID 3474020, 22 pages
https://doi.org/10.1155/2020/3474020

Research Article

Integrated Optimization on Energy Saving and Quality of Service of Urban Rail Transit System

Wenxin Li,[1] **Qiyuan Peng**,[1,2] **Chao Wen**,[1,2] **Shengdong Li**,[1] **Xu Yan**,[1] **and Xinyue Xu**[3]

[1]*School of Transportation & Logistics, Southwest Jiaotong University, Chengdu 610031, China*
[2]*National United Engineering Laboratory of Integrated and Intelligent Transportation, Southwest Jiaotong University, Chengdu 610031, China*
[3]*State Key Laboratory of Rail Traffic Control and Safety, Beijing Jiaotong University, Beijing 100044, China*

Correspondence should be addressed to Chao Wen; wenchao@swjtu.cn

Received 21 July 2019; Revised 18 October 2019; Accepted 25 October 2019; Published 3 January 2020

Academic Editor: Luca D'Acierno

Optimizing to increase the utilization ratio of regenerative braking energy reduces energy consumption, and can be done without increasing the deviation of train running time in one circle. The latter entails that the train timetable is upheld, which guarantees that the demand for passenger transport services is met and the quality of services in the urban rail transit system is maintained. This study proposes a multi-objective optimization model for urban railways with timetable optimization to minimize the total energy consumption of trains while maximizing the quality of service. To this end, we apply the principles and ideas of calculus to reduce the power of the velocity in the train energy consumption model. This greatly simplifies the complexity of the optimization model. Then, considering the conflicting requirements of decision-makers, weight factors are added to the objective functions to reflect decision-makers' preferences for energy-saving and the quality of service. We adopt the nondominated sorting genetic algorithm-II (NSGA-II) to solve the proposed model. A practical case study of the Yizhuang urban railway line in Beijing is conducted to verify the effectiveness of the proposed model and evaluate the advantages of the optimal energy saving timetable (OEST) in comparison to the optimal quality of service timetable (OQOST). The results showed that the OEST reduced total energy consumption by 8.72% but increased the deviation of trains running time in one circle by 728 s. The total energy consumption was reduced by 6.09%, but there was no increase in the deviation of train running time in one circle with the OQOST.

1. Introduction

Urban rail transit systems are playing an increasingly important role in the process of urban development. Urban rail systems provide fast, convenient, safe, and comfortable transportation services for a growing number of passengers and also help to alleviate urban traffic congestion problems. In Beijing, by the end of December 2018, the urban rail transit network included 24 lines, 388 stations, and 605 km of track in operation (data from Beijing Metro official website) and prevented over-congestion of roads due to urban traffic demand. Moreover, compared to road traffic, rail transit systems are more environmentally friendly. Therefore, rail transit systems have become an essential mode of urban transportation and are thus undergoing rapid construction and development. In a given urban rail transit system, more than 40% of the total electric energy is consumed in the train moving process, and this is affected by driving strategy and utilization of regenerative braking energy [1]. The maximum operating speed differs according to driving strategy and interval running times in urban railway, and this also affects the energy consumption of train traction. Furthermore, the utilization of regenerative braking energy is affected by train driving strategies. Generally, urban railway trains have three moving phases including accelerating, coasting, and braking. When multiple trains run consecutively in the sections served by two transformer substations, the regenerative braking energy is produced during the braking phase of the subsequent trains and consumed by the preceding train during the accelerating phase, simultaneously. Therefore, optimizing the

simultaneous moving process of urban trains can reduce any unnecessary energy-consumption in urban rail transit systems. Optimal train operation strategy aims to minimize total energy consumption by determining the dwelling time at stations between consecutive trains, which is closely related to urban train timetabling.

With the widespread application of regenerative braking technology in the urban rail system, energy-efficient timetables, which not only save energy but also are better suited to practical operations, are vitally necessary to improve train operations. Traditionally, academic research has focused on optimizing train driving strategy and establishing mathematical models to identify optimized driving strategies. These studies used numerical algorithms to solve the model and applied simulation approaches to obtain train driving strategies. Some researchers do not take the regenerative braking energy into account and thus, fail to optimize train driving strategies [2–4]. Others have adopted regenerative braking energy to improve timetabling, but there is still a lack of a detailed energy-saving operation optimization model [5–7]. We argue that the main issue in saving energy when multiple subsequent trains are running is to improve the utilization of regenerative braking energy. In this problem, we do not consider a particular train operating strategy as the main factor influencing total energy consumption. Instead, we formulate an urban train energy-saving timetable optimization method to optimize dwelling time at stations, taking the energy-saving interaction process between following trains into account. Besides, timetable changes may reduce the quality of transport services. Consequently, we present a multi-objective optimization model that reduces the total energy consumption while maintaining the quality of service.

1.1. Literature Review. Train operation strategies can affect energy consumption, which is dependent on timetable and train speed. The maintenance of energy-efficient operations for trains by establishing optimal models and using mathematical algorithms to seek optimal driving strategies has received much attention and widespread application in urban rail systems operations [8].

Initially, researchers began to apply mathematical optimization techniques to solve energy efficiency issues in driving strategies. Some works were related to minimizing energy consumption, while other works focused on optimizing driving strategy. Higgins et al. [9] proposed a biobjective optimization model to minimize the delay time and fuel consumption. Yang et al. [10] formulated an anticipated value programming model to optimize overall passenger traveling time and train delay time, where commuter passengers boarding or alighting at train stations were assumed to be fuzzy variables. Howlett [11] considered speed limits, traction efficiency, and track gradients, which can help to shape train driving, and proposed a completely analytical approach for determining the optimal driving strategy.

Also, some research studies began to pay attention to regenerative braking energy, which plays a significant role in the creation of energy-saving driving strategies. Ramos [12] proposed a timetable optimization model to maximize regenerative braking energy by increasing the overlapping time between the accelerating time of the train i and the braking time of the train $^{(i+1)\%}$ in two consecutive transformer substations. Fournier et al., Nasri et al., and Li and Yang [13–15] designed a mathematical model and employed a numerical algorithm to improve the utilization ratio of regenerative braking energy. Sun et al. [16] presented a biobjective model to minimize waiting time and energy consumption base on real-world smart card data. Then, they conducted a case study using a genetic algorithm (GA) search in the Beijing subway system. By introducing stop-skipping patterns before applying timetable optimization, the results show that the proposed model can reduce passenger waiting time and improve energy efficiency. To build on these results, we not only construct a mathematical model and numerical algorithm but also propose a set of analytical solution equations in this study.

Some researchers have also paid attention to speed profile optimization, which helps to reduce energy consumption. Bocharnikov et al. [17] proposed a single train speed profile optimization aggregation model, which considered both the tractive energy consumption and the utilization of regenerative braking energy. Furthermore, they performed a simulation experiment to prove that their aggregation model effectively minimized energy consumption. Rodrigo et al. [18] designed an algorithm to solve issues in an energy-saving driving optimization model and improve the utilization ratio of regenerative braking energy. Tuyttens et al. [19] designed a genetic algorithm to solve the complex optimization model and presented a new method to solve such optimization problems. Wang and Goverde [20] developed an optimization model that considered time and speed constraints derived from the timetable in order to calculate the minimum energy consumption of the train when it was delayed. Luan et al. [21] study energy-efficient train operation and introduce two objectives: energy consumption and delay recovery. Then, they also consider the utilization of regenerative braking energy and construct linear formulations for calculating the same. Furthermore, they use the weighted method to balance the two objective functions. The Dutch Railway was selected as a practical case to verify the effectiveness of the proposed optimization model, and the results show that train energy consumption and delay recovery time can be effectively reduced. Huang et al. [22] proposed a data-driven optimization model to describe the relationship between energy consumption and speed profile. They then integrated two typical machine learning algorithms, random forest regression (RFR), and support vector machine regression (SVR) into a heuristic algorithm to solve the model.

Not all researchers have paid attention to speed profile optimization, and many scholars use train timetabling optimization to solve problems of train energy consumption. Yin et al. [23] proposed an integrated approach and an approximate dynamic programming approach for train scheduling problems in a bidirectional urban metro line in order to minimize the operational costs (i.e., energy consumption) and passenger waiting time. Scheepmaker et al. [24] provided an extensive literature review regarding energy-efficient train control and the related topic of energy-efficient train timetabling. This area of study includes advanced models and algorithms from the last decade that deal with varying gradients,

speed limits, and regenerative braking along with energy-efficient driving strategies for a train under different conditions. Ye and Liu [25] proposed a novel and effective approach to solve several complex train control problems, including optimal control for a fleet of interacting trains and optimal train control involving scheduling. Yang et al. [26] developed a scheduling approach to coordinate the arrivals and departures of all trains located under the same electricity supply interval so that the energy regenerated from train braking could be more effectively utilized for train acceleration. Miyatake and Ko [27] introduced three methods of solving the problem of minimizing train energy consumption: dynamic programming (DP), the gradient method, and sequential quadratic programming (SQP). Yang et al. [28] developed an energy-efficient rescheduling approach to minimize net energy consumption and train delays. Then, they present an integer programming model and design an allocation algorithm to obtain the optimal schedule. Hou et al. [29] presented a mixed integer programming model to solve the metro train timetable rescheduling problem, which jointly optimizes the energy consumption and the total train delay. They solved the proposed model by using the CPLEX programming system, which can obtain trade-off solutions in a short time. Chevrier et al. [30] used the energy efficient rescheduling approach to minimize energy consumption and adopt a multi-objective evolutionary algorithm to seek the optimized solutions of the running time.

After investigating the existing literature, most of them [20–22, 26, 28, 29] have contributed to energy-efficient driving using the timetable optimization method to obtain energy-saving timetables that are conducive to reducing energy consumption. The decision variables selected in the existing literature on train energy-saving driving optimization are usually running time [20–22] or dwelling time [26, 28, 29]. The decision variable chosen in this paper is the dwelling time.

Most of the literature focuses on how to improve the utilization ratio of regenerative braking energy and reduce the total energy consumption of train operation. Few scholars consider the impact of optimization results on the quality of service. By contrast, this study considers both energy consumption and the quality of service. Table 1 shows the main research contents and contributions of energy-saving driving papers in recent years. To provide a clear comparison, we list the detailed characteristics of some closely related studies in Table 1, including decision variables, objectives, solution methods, and the complexity of the model. (We use the highest power of the decision variables in the model to represent the complexity of the model. Generally, the higher the power of the decision variables in the model, the more complex the model is.)

In summary, most of the literature in Table 1 focuses on improving energy efficiency through speed optimization [17, 20, 22] or timetable optimization [8, 15, 30]. Some studies also consider the impact of transport service quality [13, 16, 21]. Furthermore, Table 1 shows that the current solution methodologies to solve energy efficiency problems can be divided into three categories: commercial optimization software [20, 29], heuristic algorithms [8, 16, 26], and simulation methods [17]. The optimization models applied in the studies listed in Table 1 are very complex. Many of these scholars focused their efforts on producing innovative algorithms to identify an appropriate solution at a faster rate, rather than on model simplification.

This study focuses on the design and simplification of models. The energy theorem and the principles and ideas of calculus are utilized to simplify the model further. The simplified model makes it easier to calculate and obtain an appropriate solution for an energy-saving timetable. Besides, it can be seen from Table 1 that the highest power of the velocity of the model in this paper is the lowest, and this is one of the most important contributions of the modeling method and solution efficiency. Besides, extant literature mainly studies speed profile optimization and train timetabling optimization to reduce the energy consumption of trains. Few studies have considered the impact of timetable optimization on the quality of service. Therefore, this study proposes a multi-objective programming optimization model, which considers both energy consumption and the quality of service. The complex optimization model is simplified by using the principles and ideas of calculus and energy theorems. Furthermore, this study applies a non-dominated sorting genetic algorithm-II (NSGA-II) to minimize the total energy consumption of trains while maximizing the quality of service. Thus, this study fills a gap in the academic literature.

1.2. Objective and Contributions. Generally, energy-saving train operation strategies consider three operation phases for a complete trip between two stations for a single train. Thus, first, we analyze the usual driving process for a single train and present the appropriate motion equations for this situation. The concept of regenerative braking energy is proposed on the basis of the three operation phases for a single train driving process. This allows for the optimization of the simultaneous and interactive moving processes between multiple urban trains. The analytical calculation equations for regenerative braking energy are formulated in accordance with the applicable principles that govern the electric energy transmission interaction processes between trains. Subsequently, we integrate the concept of the regenerative braking energy into the optimization solutions for urban rail transit systems' timetabling and present a simplified energy consumption calculation model. The calculation model for the optimization problem for train-following should minimize the total energy consumption of one train while increasing the simultaneous interaction moving the process of subsequent trains in order to improve the effectively utilized regenerative braking energy ratio. This ratio is represented by η, and η is positively correlated with overlapping time, so increasing the overlapping time period is important. We also consider and construct the objective function to determine the quality of service to ensure that our energy-saving optimization timetable maintains a high quality of service.

To exemplify the validity of this method, it is applied to the Yizhuang urban rail line in Beijing, China. Thus, the theoretical and practical contributions of the study are as follows:

Table 1: Recent publications on energy-saving driving in comparison with this study.

Publication	Decision variable		Objects		The highest power of the velocity		Solution methods
	Timetable	Speed profiles	Energy consumption	The quality of service	<3	>=3	
Li and Lo (2014)	√	√	√			√	GA
Fournier et al. (2012)	√		√	√		√	Linear programming algorithm
Nasri et al. (2010)	√		√			√	GA
Li and Yang (2013)	√		√			√	A binary-coded genetic algorithm
Bocharnikov et al. (2010)		√	√			√	GA
Rodrigo et al. (2013)		√	√			√	Semi-analytical solution
Tuyttens et al. (2013)		√	√			√	GA
Sun et al. (2019)	√		√	√		√	GA
Chevrier et al. (2013)	√		√			√	Multi-objective evolutionary algorithm
Wang and Goverde (2016)		√	√			√	Pseudospectral method
Luan et al. (2018)		√	√	√		√	PNLP approach and the PTSPO approach
Huang et al. (2019)		√	√			√	Machine learning algorithms
Yin et al. (2016)	√		√	√		√	Dynamic programming algorithm
Ye and Liu (2017)		√	√			√	Two novel methods
Yang et al. (2015)	√		√			√	GA
Yang et al. (2019)	√		√	√		√	Allocation algorithm
Hou et al. (2019)	√		√	√		√	CPLEX
This paper	√		√	√	√		NSGA-II

(1) We present a multi-objective optimization model to reduce the total energy consumption and increase the quality of service of urban rail transit systems.

(2) The energy consumption model was simplified using the principles and ideas of calculus and the analytical solution equations.

(3) The NSGA-II algorithm was adopted to solve the model effectively.

(4) The effectiveness of the proposed model was exemplified in a practical case study.

The rest of this paper is organized as follows. In Section 2, we construct the multi-objective optimization model for urban rail transit systems based on regenerative braking to minimize the total energy consumption of trains while maximizing the quality of service. We adopt the NSGA-II algorithm for finding an appropriate solution to the optimized timetables in Section 3. Section 4 analyzes the Yizhuang urban rail line in Beijing as a practical case to verify the effectiveness of the optimized model and to evaluate the effect of the different optimized timetables based on the model. The conclusions are summarized in Section 5.

2. Multi-Objective Optimization Model

2.1. Notation Description. To create an appropriate model for regenerative braking energy-based operations, we apply specific indices, parameters, and variables (including decision variables) regarding train operations, as shown in Tables 2–4.

2.2. An Optimized Energy Consumption Modeling Method for a Single Train. Concerning a complete driving process for a single train, Howlett [11] defined the optimal driving phases for trains as accelerating, coasting, and braking. As shown in Figure 1, two inflection points W_1 and W_2 on the v-s curve separate the three phases of train driving. v_1 and v_2 indicate the maximum speed of an urban train at the end of its accelerating phase and its speed at the beginning of its braking phase, respectively, while s_1, s_2, and s_3 indicate the train's traveling distances during the accelerating phase, the coasting phase, and braking phase, respectively.

For this analysis, we assume that the impacts of railway line physical engineering conditions do not need to be considered. According to train motion equations, the acceleration and speed of a single train can be obtained as shown in Equations (1) and (2). a indicates acceleration, v indicates

Table 2: Index definitions.

Symbol	Descriptions
$\kappa = \{1, 2, \ldots K\}$	Set of trains index
$\Upsilon = \{1, 2, \ldots 2M\}$	Set of stations index
$\Gamma = \{1, 2, \ldots 2I\}$	Set of station sections index
$\Lambda = \{1, 2, \ldots J\}$	Set of train driving phases
i	Index of sections, $i \in \Gamma$
j	Index of phases, $j \in \Lambda$
m	Index of stations, $m \in \Upsilon$
k	Index of trains, $k \in \kappa$

Table 3: Parameter definitions.

Symbol	Descriptions
s_{kij}	The distance of phase j in the section i of train k, m
$f(v)$	The traction force characteristic curve, kN
$b(v)$	The braking force characteristic curve, kN
$r(v)$	The basic resistance characteristic curve, generally expressed as $r(v) = a_0 v^2 + b_0 v + c_0$, a_0, b_0, c_0 are constant, kN
$F_{\max}$	The maximum traction force of a train, kN
$B_{\max}$	The maximum braking force of a train, kN
$\eta_{k,i}$	The utilization ratio of regenerative braking capacity of train k in the section i
E_{mech}	The kinetic energy in the braking phase, kwh
$a_{\text{acc}}^{\max}$	The maximum acceleration, m/s^2
$a_{\text{dec}}^{\max}$	The maximum deceleration, m/s^2
ξ	The regenerative braking energy conversion rate
T_{zf}	The turn-around time at the terminal station, sec

Table 4: Variable definitions.

Symbol	Descriptions
v_{kij}	The speed of phase j in the section i of train k, m/s
t_{kij}	The time duration of phase j in the section $i$of train k, sec
E_{reg}	Regenerative braking energy, kWh
$t_{k,k+1}^{overlap}$	The interaction time or overlapping time duration between the braking phase time of train $k+1$ and the accelerating phase time of train k, sec
t_{k+1}^{brake}	The braking phase time duration of train $k+1$, sec
H_s	The headway between the subsequent trains, sec
θ_1, θ_2	$\theta_1, \theta_2 \in \{0, 1\}$ are two binary parameters with $\theta_1 \cdot \theta_2 = 0$
$D_{k,m}^{\text{cut}}$	The current dwell time of train k at station m, sec
$D_{k,m}^{\text{opt}}$	The optimized dwell time of train k at station m, sec (decision variables)

speed, t indicates time, s indicates distance, f_{total} is the resultant force of a train, and m_{total} is the total weight of an empty train.

$$a = \frac{f_{total}}{m_{total}} = \frac{\theta_1 f(v) - \theta_2 b(v) - r(v)}{m_{total}} = \frac{\mathrm{d}v}{\mathrm{d}t}, \tag{1}$$

$$v = \frac{\mathrm{d}s}{\mathrm{d}t}. \tag{2}$$

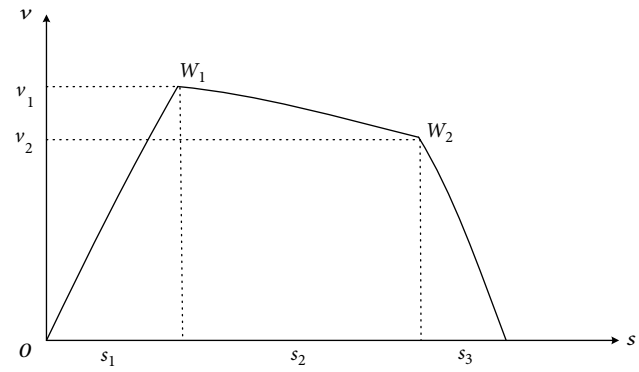

Figure 1: The v–s curve of train operations between stations.

By combining Equations (1) and (2), we can derive the dv-ds relationship Equation (3), as shown below:

$$\frac{\mathrm{d}v}{\mathrm{d}s} = \frac{\theta_1 f(v) - \theta_2 b(v) - r(v)}{v}. \tag{3}$$

Furthermore, the duration of the three phases and the distance of train driving can be derived through the dv-ds relationship Equation (3) under different operation situations. Equations (4)–(9) can be deduced from Equations (1)–(3). In the train's acceleration phase, the traction force is greater than its basic and extra resistance forces, thus speeding it up until it runs at the maximum speed, v_1. The running time, t_1, and distance, s_1, can be calculated using Equations (4) and (5):

$$t_1 = \int_0^{v_1} \frac{1}{f(v) - r(v)} \mathrm{d}v, \tag{4}$$

$$s_1 = \int_0^{v_1} \frac{v}{f(v) - r(v)} \mathrm{d}v. \tag{5}$$

There is no effect from the traction force and braking force during the train's coasting phase. The running time, t_2, and distance, s_2, can be calculated using Equations (6) and (7):

$$t_2 = \int_{v_1}^{v_2} \frac{1}{-r(v)} \mathrm{d}v, \tag{6}$$

$$s_2 = \int_{v_1}^{v_2} \frac{v}{-r(v)} \mathrm{d}v. \tag{7}$$

Finally, during the braking phase, the braking force works to decelerate the train and make it stop. The running time, t_3, and distance, s_3, can be calculated using Equations (8) and (9):

$$t_3 = \int_{v_2}^{0} \frac{1}{-b(v) - r(v)} \mathrm{d}v, \tag{8}$$

$$s_3 = \int_{v_2}^{0} \frac{v}{-b(v) - r(v)} \mathrm{d}v. \tag{9}$$

Therefore, the energy consumption for the operation of a single train in each section of the trip can be calculated using Equation (10). However, traction only works during

the first phase, and the traction force's effect is mainly to increase the kinetic energy of trains. The rest is used to overcome the basic resistance of the rail line. Therefore, Equation (10) can be rewritten for the first phase as shown in Equation (11).

$$E_i = \sum_{i\in\Gamma}\sum_{j=1}^{3}\int_0^{s_{ij}} f(v)\cdot \mathrm{sd}s, \tag{10}$$

$$E_i = W_{\mathrm{tra}} = \frac{1}{2}m_{total}v_{i1}^2 + \int_0^{s_{i1}} r(v)\cdot \mathrm{sd}s. \tag{11}$$

The braking force only works in the third phase, and the braking force's effect mainly decreases the kinetic energy of the train until it reaches a value of 0. The braking force is also a resistance force, similar to the basic resistance of the rail line. As shown in Equation (12).

$$W_{\mathrm{bra}} = \frac{1}{2}m_{total}v_{i2}^2 - \int_0^{s_{i3}} r(v)\cdot \mathrm{sd}s. \tag{12}$$

We assume that the ratio of the traction force's effect on the basic resistance's effect during the accelerating phase in each section is ω_{t}. Furthermore, we assume that the ratio of the braking force's effect on the basic resistance's effect during the braking phase in each section is ω_{b}. Under these conditions, Equations (11) and (12) can be re-written as Equations (13) and (14), respectively.

$$E_i = W_{\mathrm{tra}} = \left(1 + \frac{1}{\omega_{\mathrm{t}}}\right)\cdot\frac{1}{2}m_{total}v_{i1}^2, \tag{13}$$

$$W_{\mathrm{bra}} = \frac{\omega_{\mathrm{b}}}{1+\omega_{\mathrm{b}}}\cdot\frac{1}{2}m_{total}v_{i2}^2. \tag{14}$$

According to the calculation method of power and energy, as shown in Equation (15), the calculation method of ω_{t} and ω_{b} can be written as Equation (16).

$$\left.\begin{array}{c} W = Pt \\ W = FS = Fvt \end{array}\right\} \Longrightarrow P = Fv, \tag{15}$$

$$\begin{aligned}
\omega_{\mathrm{t}} &= \frac{W_{\mathrm{tra}}}{W_{\mathrm{res}}} = \frac{\int_0^{s_{i1}} f(v)\cdot \mathrm{sd}s}{\int_0^{s_{i1}} r(v)\cdot \mathrm{sd}s} = \frac{\int_0^{v_{i1}} f(v)\cdot s\cdot t\mathrm{d}v}{\int_0^{v_{i1}} r(v)\cdot s\cdot t\mathrm{d}v} = \frac{\int_0^{v_{i1}} f(v)\mathrm{d}v}{\int_0^{v_{i1}} r(v)\mathrm{d}v}, \\
\omega_{\mathrm{b}} &= \frac{W_{\mathrm{bra}}}{W_{\mathrm{res}}} = \frac{\int_0^{s_{i3}} b(v)\cdot \mathrm{sd}s}{\int_0^{s_{i3}} r(v)\cdot \mathrm{sd}s} = \frac{\int_0^{v_{i2}} b(v)\cdot s\cdot t\mathrm{d}v}{\int_0^{v_{i2}} r(v)\cdot s\cdot t\mathrm{d}v} = \frac{\int_0^{v_{i2}} b(v)\mathrm{d}v}{\int_0^{v_{i2}} r(v)\mathrm{d}v}.
\end{aligned} \tag{16}$$

W is the energy; P is the power; F is the force; S is the distance; v is the speed; t is the time; W_{tra} is the traction force's effect; W_{res} is the basic resistance's effect; and W_{bra} is the braking force's effect.

Yang et al. [26] show that, if the train operates in the section with the optimal energy-saving driving strategy, the speed v_{i1} at the end of the train's accelerating phase generally reaches 54 km/h but does not exceed 72 km/h and the speed v_{i2} at the beginning of the train's braking phase generally reaches 46 km/h but does not exceed 60 km/h. After referring to the data resources of Li et al. [31], Figure 2 shows the relationships between traction, basic resistance, and braking force. Finally,

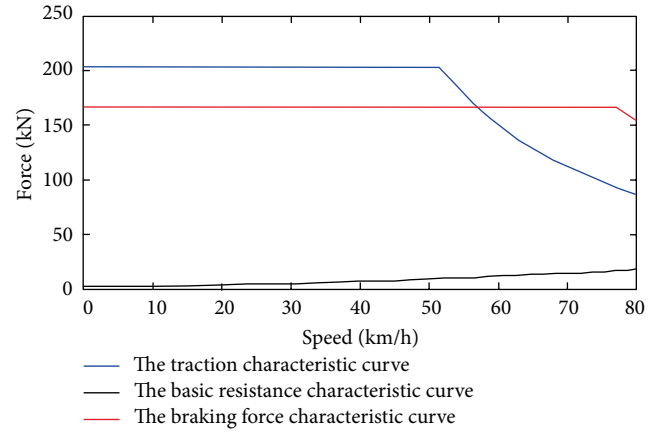

Figure 2: The traction, basic resistance, and braking force characteristic curves.

we can derive $1/\omega_{\mathrm{t}} \in [r(54)/f(54), r(72)/f(72)]$ and $1/\omega_{\mathrm{b}} \in [r(46)/f(46), r(60)/f(60)]$ (as shown in Figures 3 and 4). Figure 3 shows the integral values of traction force and basic resistance with the velocity at 54 km/h and 72 km/h, respectively. Furthermore, Figure 4 shows the integral values of braking force and basic resistance with the velocity at 46 km/h and 60 km/h, respectively.

Finally, we use the integral function "quad" of MATLAB to calculate $f(54), r(54), f(72), r(72), f(46), r(46), f(60)$, and $r(60)$. We obtain $1/\omega_{\mathrm{t}} \in [295.2/10938.8, 532.3/13451.1]$ and $1/\omega_{\mathrm{b}} \in [217.9/7636, 532.3/9960]$. Therefore, the traditional energy consumption model of a single train (Equation 10) can be simplified to Equation (17). In order to make Equation (17) correct, it must satisfy the following three premises.

(1) The object is the urban rail transit system so the maximum speed of trains should not exceed 80 km/h, the maximum train acceleration is equal to 1 m/s^2, and the maximum train deceleration is equal to -1 m/s^2.

(2) The distance between each station should not exceed 3 kilometers in principle, and the train movement in each section consists of only three phases: accelerating, coasting, and braking.

(3) The traction, basic resistance, and braking force characteristic curves are given. Their values in this study are shown in Figure 2.

$$E_i = \frac{\omega_{\mathrm{t}}+1}{2\omega_{\mathrm{t}}}m_{total}v_{i1}^2. \tag{17}$$

2.3. Application of Regenerative Braking Energy between Multiple Trains. Regenerative braking technology is an energy-saving approach that converts the kinetic energy in a train's braking phase into electric energy (i.e., regenerative braking energy). This electric energy is transmitted to another train during the acceleration phase. The transformer substation is the main electricity source that supports running trains. Specifically, when multiple trains run consecutively in the sections served

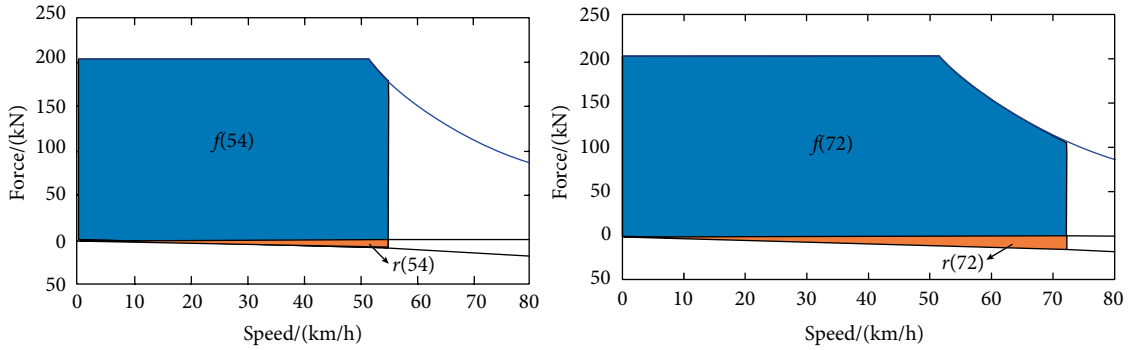

Figure 3: Integral diagram of traction force (blue line) and basic resistance (black line).

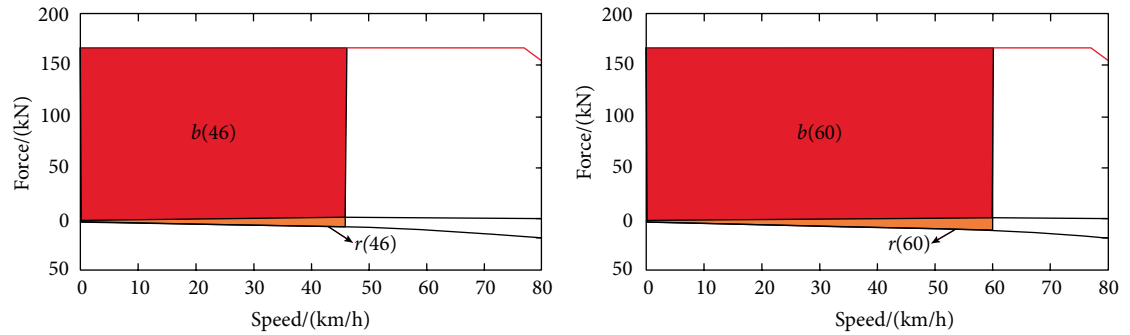

Figure 4: Integral diagram of braking force (red line) and basic resistance (black line).

by two transformer substations, the motor of the subsequent train switches to generator mode to convert kinetic energy from the braking phase into regenerative braking energy, while regenerative braking energy is simultaneously transmitted to the same power supply section, to accelerate the preceding train in the accelerating phase. Therefore, optimizing this simultaneous interaction moving process between urban trains can recycle kinetic energy and thus, reduce the energy consumption of urban rail transit systems. This optimal train driving strategy aims to minimize total energy consumption by determining dwelling time, which is closely related to urban train timetabling.

Let us assume that there are N trains running under two transformer substations and that these N trains are sorted as $k, k+1, \ldots, k+N+1$. The focus of our research is to maximize the utilization of regenerative braking energy. In other words, the regenerative braking energy produced by any train during its braking phase can be best absorbed and utilized by other trains in traction phases in the two transformer substations. As shown in Figure 5, the solid arrows indicate the direction of electricity transmission. The train $k+1, \ldots, k+N+1$ will convert kinetic energy into regenerative braking energy, E_{reg}, during the braking phase. The preceding train, k, in its accelerating phase, can utilize E_{reg} and save the electric energy obtained from the transformer substation. Train $k+1, \ldots, k+N+1$ in its braking phase can produce regenerative braking energy, most of which will be wasted as heat energy if there is no other train running in two consecutive transformer substations. Only a small part of the regenerative braking energy can be utilized to support air conditioning, lighting, and other equipment.

As described above, regenerative braking energy is the converted energy derived when the energy of overcoming resistance forces is subtracted from the kinetic energy in transit operations involving multiple trains.

$$\begin{aligned} E_{reg} &= \left(E_{\text{mech}} - W_{\text{res}}\right) \cdot \xi \\ &= \left(\frac{1}{2} m_{total} v_{i2}^2 - W_{\text{res}}\right) \cdot \xi \\ &= W_{\text{bra}} \cdot \xi, \end{aligned} \tag{18}$$

where E_{mech} is the kinetic energy and W_{res} is the basic resistance's effect.

The effective utilization of regenerative braking energy by train k, which is generated by train $k+1, \ldots, k+N-1$ during braking phases as shown in Figure 6, can be calculated as follows:

$$\begin{aligned} E_{used} &= E_{reg} \cdot \eta \\ &= W_{\text{bra}} \cdot \xi \cdot \left(\frac{t_{k,k+1}^{overlap}}{t_{k+1}^{brake}} + \frac{t_{k,k+2}^{overlap}}{t_{k+2}^{brake}} + \cdots + \frac{t_{k,k+N-1}^{overlap}}{t_{k+N-1}^{brake}} \right). \end{aligned} \tag{19}$$

η is the utilization ratio of regenerative braking energy. The effectively utilized ratio, η, directly determines how much electric energy can be saved by utilizing regenerative braking energy. The regenerative braking energy generated by train $k+1, \ldots, k+N-1$ in its braking phase is directly proportional to the overlapping time between the braking phase time

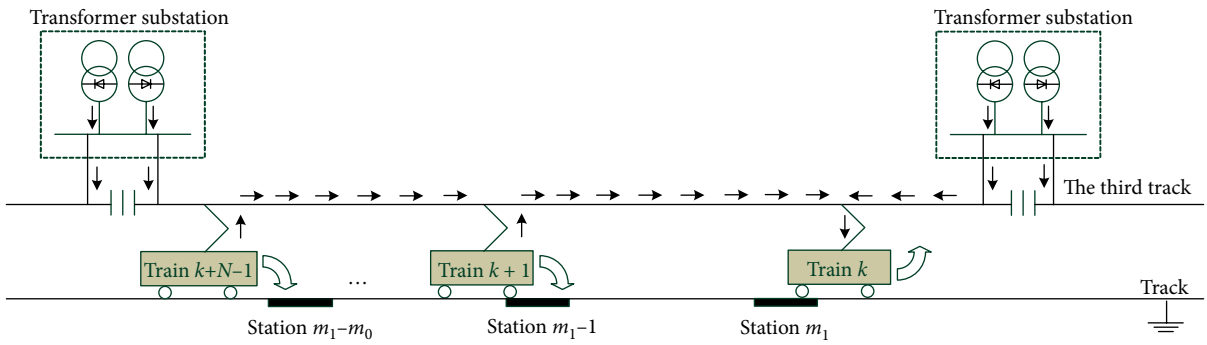

FIGURE 5: A schematic of regenerative braking energy utilization. Note: Figure 5 imitates the drawing style of [26].

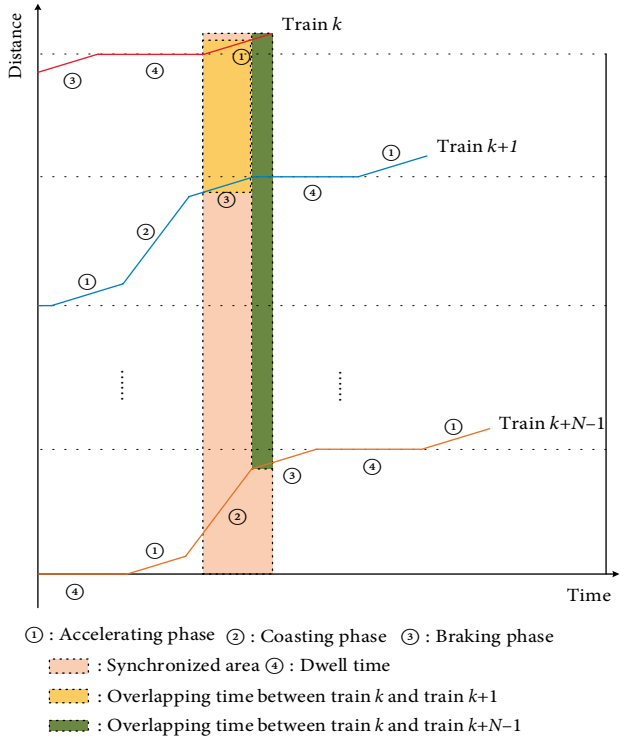

FIGURE 6: The diagram of regenerative braking energy utilization of train k.

of the subsequent trains and the accelerating phase time of train k.

The start time of the accelerating phase of the preceding train k's departure from station m_1 can be used as a basic reference time. At the reference time, the operation time of train k is t_k, the operation time of train $k+1$ is t_{k+1}, and so on. Furthermore, the operation time of the train $k+N-1$ is t_{k+N-1}, as Equations (20)–(22) show.

$$t_k = \sum_{i=1}^{m_1-1} \sum_{j=1}^{3} t_{ij} + \sum_{m=2}^{m_1} D_{k,m}^{\text{opt}}, \tag{20}$$

$$t_{k+1} = \sum_{i=1}^{m_1-2} \sum_{j=1}^{3} t_{ij} + \sum_{m=2}^{m_1-2} D_{k+1,m}^{\text{opt}} - t_{m_1-2,3} - \Delta_{k+1}, \tag{21}$$

$$t_{k+N-1} = \sum_{i=1}^{m_1-m_0-1} \sum_{j=1}^{3} t_{ij} + \sum_{m=2}^{m_1-m_0-1} D_{k+N-1,m}^{\text{opt}} - t_{m_1-m_0-1,3} - \Delta_{k+N-1}. \tag{22}$$

Δ_{k+1} is the deviation time when train $k+1$ enters the braking phase in the running section, Δ_{k+N-1} is the deviation time when train $k+N-1$ enters the braking phase in the running section, and $(\Delta_{k+1}, \Delta_{k+2}, \cdots, \Delta_{k+N-1})$ is a group of small, positive numbers.

In order to maximize regenerative braking energy and ensure that the regenerative braking energy produced by the subsequent trains is fully utilized by train k, we assume that $\eta = 1$. As Equation (23) shows,

$$\frac{t_{k,k+1}^{overlap}}{t_{k+1}^{brake}} + \frac{t_{k,k+2}^{overlap}}{t_{k+2}^{brake}} + \cdots + \frac{t_{k,k+N-1}^{overlap}}{t_{k+N-1}^{brake}} \geq 1. \tag{23}$$

Assuming $t_{k+N_1}^{brake} = \min\left(t_{k+1}^{brake}, t_{k+2}^{brake}, \ldots, t_{k+N-1}^{brake}\right)$, Equation (23) can be derived as follows:

$$\begin{aligned} &\frac{t_{k,k+1}^{overlap}}{t_{k+N_1}^{brake}} + \frac{t_{k,k+2}^{overlap}}{t_{k+N_1}^{brake}} + \ldots + \frac{t_{k,k+N-1}^{overlap}}{t_{k+N_1}^{brake}} \geq 1, \\ &t_{k,k+1}^{overlap} + t_{k,k+2}^{overlap} + \ldots + t_{k,k+N-1}^{overlap} \geq t_{k+N_1}^{brake}. \end{aligned} \tag{24}$$

Equation (25) shows the maximum overlapping time between the braking phase time of the subsequent trains and the accelerating phase time of train k. Equation (25) shows,

$$\begin{aligned} t_{k,k+1}^{overlap} &= t_{m_1,1} - \Delta_{k+1}, \\ t_{k,k+2}^{overlap} &= t_{m_1,1} - \Delta_{k+2}, \\ t_{k,k+N-1}^{overlap} &= t_{m_1,1} - \Delta_{k+N-1}. \end{aligned} \tag{25}$$

Therefore, Equation (24) can be written as follows:

$$\begin{aligned} &t_{m_1,1} - \Delta_{k+1} + t_{m_1,1} - \Delta_{k+2} + \cdots + t_{m_1,1} - \Delta_{k+N-1} \geq t_{k+N_1}^{brake}, \\ &(N-1)t_{m_1,1} - \left(\Delta_{k+1} + \Delta_{k+2} + \cdots + \Delta_{k+N-1}\right) \geq t_{k+N_1}^{brake}. \end{aligned} \tag{26}$$

Based on Equation (26), Equation (24) can be rewritten as follows:

$$\frac{t_{m_1,1}}{t_{k+N_1}^{brake}} + \frac{(N-2)t_{m_1,1} - \left(\Delta_{k+1} + \Delta_{k+2} + \cdots + \Delta_{k+N-1}\right)}{t_{k+N_1}^{brake}} \geq 1. \tag{27}$$

According to the results of relevant literature [27, 30], we know that the duration of the acceleration phase is generally longer than the duration of the braking phase: $\left(t_{m_1,1}/t_{k+N_1}^{brake}\right) \geq 1$. Therefore, in order to ensure the validity of Equation (27), Equation (27) only needs to satisfy $(N-2)t_{m_1,1} - \left(\Delta_{k+1} + \Delta_{k+2} + \cdots + \Delta_{k+N-1}\right) = 0$. Furthermore, we can obtain many feasible solutions to ensure the validity of $(N-2)t_{m_1,1} - \left(\Delta_{k+1} + \Delta_{k+2} + \cdots + \Delta_{k+N-1}\right) = 0$ by adjusting the train timetable. However, the optimal solution must be calculated using the optimization theory. Equation (27) only provides an optimization direction for the model.

2.4. Establishment of Analytical Solution Equations. As discussed above, the key to improving energy-consumption efficiency is to increase the effectively utilized regenerative braking energy ratio, which is represented by η, where η is positively correlated with overlapping time. Thus, increasing the overlapping time period is important. The optimal overlapping time duration $\left(t_{k,k+1}^{overlap}, t_{k,k+2}^{overlap}, ..., t_{k,k+N-1}^{overlap}\right)$ is affected by many elements, including headways between trains and train dwelling times at stations, which makes the model solution highly complex. Based on the systematic analysis of processes involving subsequent trains, we constructed a set of analytical solution equations to reduce the difficulty of solving the problem.

First, the precondition for the interaction processes of subsequent trains to produce regenerative braking energy is that the subsequent trains should run in the sections of two transformer substations. The most common and simple case is where two trains run in consecutive sections. Theoretically and practically, multiple trains can run in two transformer substations. Generally, the length of headway H_s (i.e., the tracking time interval between subsequent trains) determines the number of sections and stations between subsequent trains. In essence, improving the interaction processes between subsequent trains involves changing the dwelling time at stations between them to increase the effective overlapping time between them. Based on the analysis provided above, the analytical solution equations are constructed, while also considering the different numbers of stations between the subsequent trains.

In addition, we know that the headway of two subsequent trains will be constant in the same period, as $t_k - t_{k+1} = t_{k+1} - t_{k+2} = ... = t_{k+N-2} - t_{k+N-1} = H_s$, and the accelerating phase is generally longer than the braking phase. In order to analyze the optimal interaction processes of subsequent trains, we present a set of analytical solution equations to express the optimal interaction process between them. According to these equations, the regenerative braking energy produced by the subsequent trains in the braking phase can be fully consumed by the preceding train in its accelerating phase, as shown in Equations (28)–(30). According to the analysis results of Equation (27), we know that when we obtain a set data of $\left(\Delta_{k+1}, \Delta_{k+2}, \cdots, \Delta_{k+N-1}\right)$, we can calculate the dwelling time at stations between subsequent trains using Equations (28)–(30). Thus, when we obtain a set of optimized data $\left(\Delta_{k+1}, \Delta_{k+2}, \cdots, \Delta_{k+N-1}\right)$, we can calculate the optimal dwelling time at stations between the subsequent trains.

$$H_s - D_{k,m_1}^{\text{opt}} - \sum_{i=m_1-1}^{\sum} \sum_{j=1}^{3} t_{ij} - D_{k+1,m_1-1}^{\text{opt}} = t_{m_1-2,3} + \Delta_{k+1}, \tag{28}$$

$$2H_s - D_{k,m_1}^{\text{opt}} - \sum_{i=m_1-2}^{m_1-1} \sum_{j=1}^{3} t_{ij} - D_{k+1,m_1-1}^{\text{opt}} - D_{k+2,m_1-2}^{\text{opt}} = t_{m_1-3,3} + \Delta_{k+2}, \tag{29}$$

$$(N-1)H_s - \left(D_{k,m_1}^{\text{opt}} + D_{k+1,m_1-1}^{\text{opt}} + \cdots + -D_{k+N-1,m_1-N+1}^{\text{opt}}\right) - \sum_{i=m_1-N+1}^{m_1-1} \sum_{j=1}^{3} t_{ij} = t_{m_1-N,3} + \Delta_{k+N+1}. \tag{30}$$

In summary, the analytical solution equations can obtain the ranges of dwelling times to fully utilize the regenerative braking energy and also largely reduce the solving efforts required to obtain acceptable solutions.

2.5. Objective Functions and Constraint Conditions. Based on the aforementioned train motion equations and regenerative braking energy principles, the mathematical model for the timetable optimization aims to minimize the total energy consumption of trains, while maximizing the quality of service. Furthermore, we have considered that the change of dwelling time will have a certain impact on passengers alighting/boarding the train. Therefore, in order to avoid this problem, firstly, we limit the scope of application of this optimization model, which stipulates that the scope of application of this optimization model is during the nonpeak hours of metro operation (the headway of the case selected in this paper is 210 s), even during the low-peak period of passenger travel at night, because the passenger flow is relatively low during these two periods, so the reasonable change of dwelling time will have less impact on passengers alighting/boarding the train. Secondly, we set upper and lower limits of dwelling time, which can let the solution more make sense, as shown in Table 5. The upper and lower limits of dwelling time are the specific values given by Beijing Metro considering the actual passenger transport demand during the nonrush hours. Therefore, we think that optimizing the dwelling time within a reasonable range of values will have less impact on passengers alighting/boarding the train.

Not at all, the reasonable dwell time should be certainly considered when optimizing the timetable with the target of minimizing energy consumption, and that is why we establish the integrated optimization on energy saving and quality of service, in which the stability and robustness of the timetable against disruption should be carefully considered. We want to obtain timetables that can reach a balance between the energy-saving and service quality by taking into account the dwell time as an important factor. Also, we believe that train delay recovery and adjustment can be studied as an independent issue because the location of delay and the initial delay time will affect the choice of delay recovery strategy, so the problem of delay recovery and adjustment is also a complex optimization problem. However, the main purpose of this paper is to minimize energy consumption and maximize the quality of

Table 5: Other parameters used in the model.

m_{totol}/kg	$D_{\min}$/s	$D_{\max}$/s	L_{limit}/m	ξ	T_{zf}/s	T_{total}/s	H_s/s	a_0	b_0	c_0
194295	20	45	100	0.90	300	6800	210	0.001807	0.0622	2.031

services by optimizing reasonable train dwelling time. This paper does not consider the study of train delay recovery. So we set an upper and lower limit of dwelling time to let the resolutions make more sense, as shown in Table 5. The upper and lower limits of dwelling time are the specific values given by Beijing Metro considering the actual passenger transport demand during the nonrush hours. Reasonable dwelling time setting can help this paper avoid considering delayed recovery.

We use E_{total} to express the total energy consumption of trains. Based on the analysis in Section 2.2, which applied calculus to simplify the calculation model of train energy consumption, the complexity of the objective function E_{total} has been reduced. The formulation of the metro train timetables takes many factors into account, such as passenger transport plan, energy-saving, and so on. So the current timetable is the timetable that best meets the quality of service. In this study, we use ε_{total}, which represents the deviation between the total running time of all trains in one circle under the optimized timetable and the total running time of all trains in one circle under the current timetable, to express the difference between the optimized timetable and the current timetable. When ε_{total} is large, we believe that the optimized timetable does not have the same characteristics as the current timetable, which means that the demand of passenger transport services is not met. For the operation enterprises, it means that the punctuality rate of train operation decreases, and for the passengers, it means that the quality of transport services decreases. When ε_{total} is small, we conclude that the optimized timetable has the same characteristics as the current schedule. Furthermore, according to the research results of Yang et al. [26], in order to maintain the quality of the passenger transport service (quality of service), the total running time of a train in one circle under the optimized timetable should be the same as the total running time of a train in one circle under the current timetable. Therefore, we use ε_{total} to express the quality of the service in the context of the research in this study. Since the decision variable in this study is the dwelling time of a train at a station, and the running time of trains in sections does not change, the deviation of train running time in one circle,ε_{total}, can be expressed by Equation (32). Considering the objective function ε_{total} is only a linear model; it does not need to be further simplified. Since the objective function E_{total} has been simplified, we can use NSGA-II to solve the multi-objective programming model. Besides, we set weight factors to meet the demands of different preferences of decision-makers. λ_e is the weight factor of total energy consumption, E_{total}, and λ_s is the weight factor of the total cycle time error rate, ε_{total}. According to the research results of Li et al. [31], we adopt $\lambda_e/\lambda_s = 10:1$ to reflect decision-makers' preferences for energy-saving and use $\lambda_e/\lambda_s = 1:10$ to reflect decision-makers' preferences for quality of service in this study.

$$\begin{aligned}\min \lambda_e E_{total} &= \lambda_e \left[\sum_{k=1}^{K} \sum_{i=1}^{2I} \sum_{j=1}^{J} \int_0^{s_{kij}} f(v) s \mathrm{d}s \right. \\ &\quad \left. - \sum_{k=1}^{K} \sum_{i=1}^{2I} \sum_{j=1}^{J} \int_0^{s_{kij}} b(v) s \mathrm{d}s \times \xi \times \eta_{k,i} \right] \\ &= \lambda_e \left[\sum_{k=1}^{K} \sum_{i=1}^{2I} \left(1 + \frac{1}{\omega_{\mathrm{t}}}\right) \cdot \frac{1}{2} m_{total} v_{ki1}^2 \right. \\ &\quad \left. - \sum_{k=1}^{K} \sum_{i=1}^{2I} \frac{\omega_{\mathrm{b}}}{1+\omega_{\mathrm{b}}} \cdot \frac{1}{2} m_{total} v_{ki2}^2 \times \xi \times \eta_{k,i} \right], \end{aligned} \tag{31}$$

$$\min \lambda_s \varepsilon_{total} = \lambda_s \left| \sum_{k=1}^{K} \sum_{m=1}^{2M} \left(D_{k,m}^{\mathrm{opt}} - D_{k,m}^{\mathrm{cut}} \right) \right|. \tag{32}$$

To guarantee safety and prevent the train from extreme cases of operation, the proposed optimization model should satisfy the following constraints:

First, the train operation should be restricted by dynamic constraints and kinematic constraints. Equation (33) represents dynamic constraints and Equations (4)–(9), (34)–(36) represent kinematic constraints. Considering that the basic resistance of the line $r(v)$ is known, it can be generally expressed as $r(v) = a_0 v^2 + b_0 v + c_0$. a_0, b_0, and c_0 are constant. We can calculate $f(v)$ and $b(v)$ using Equations (35) and (36):

$$\begin{aligned} 0 \le f(v) \le F_{\max}, \\ 0 \le b(v) \le B_{\max}, \end{aligned} \tag{33}$$

$$s_i = \sum_{j=1}^{J} s_{ij}, \tag{34}$$

$$0 \le \frac{f(v) - r(v)}{m_{total}} = a \le a_{\mathrm{acc}}^{\max}, \tag{35}$$

$$0 \le \frac{b(v) + r(v)}{m_{total}} = a \le \left| a_{\mathrm{dec}}^{\max} \right|. \tag{36}$$

Second, the following constraints also apply: T_{total} is the total operation time of the research period; T_i is the operation time of the train in section I; $\sum_{m=2}^{M-1} D_{k,m}$ is the total dwelling time at stations excluding the origin and destination stations in the upward direction; and $\sum_{m=M+1}^{2M-1} D_{k,m}$ is the total dwelling time at stations excluding the origin and destination stations in the downward direction. The operating time of the train in the running sections should satisfy the following constraints:

$$\sum_{i=1}^{2I} \sum_{j=1}^{J} t_{ij} + \sum_{m=2}^{M-1} D_{k,m}^{\mathrm{opt}} + \sum_{m=M+1}^{2M-1} D_{k,m}^{\mathrm{opt}} + T_{zf} + (K-1) \cdot H_s = T_{total}, \tag{37}$$

$$\sum_{i \in \Gamma} \sum_{j=1}^{J} t_{ij} = T_i. \tag{38}$$

Table 6: Comparative analysis of several major multi-objective optimization algorithms.

Algorithm	Advantage	Insufficient
NSGA	The number of optimization objectives is unrestricted, the distribution of noninferior optimal solutions is uniform, and multiple equivalent solutions are allowed to exist.	The computational efficiency is low, and the shared parameters should be determined in advance.
PAES	Using "1 + 1" strategy and local search evolutionary strategy, making its solution time lower than other algorithms.	Easy to lose the horizontal or vertical Pareto front solution.
SPEA	Using an external population to realize elite retention strategy.	Using clustering to delete individuals from the external population, which may lose the noninferior solution in the external population.
MOEA/D	The convergence rate is faster, and the computational complexity is lower. Because the weight vectors guiding evolution are uniformly distributed, the solutions obtained by MOEA/D are uniformly distributed.	When dealing with multi-objective optimization problems with high dimensions, its distribution cannot be guaranteed, and the effect is poor.
NSGA-II	Using the crowded-comparison operator and elite strategy to expand the sampling space, which allows the parents and their offspring to participate in the competition to produce the next generation of the population and generate better offspring.	When dealing with multi-objective optimization problems, congestion distance is not applicable in high-dimensional space, and computational complexity is high.

Third, $D_{k,m}^{\text{opt}}$ is the optimized dwell time of train k at station m, $D_{\min}$ and $D_{\max}$ are the lower and upper bound of the dwell time. In order to ensure efficient passenger transport, $D_{k,m}^{\text{opt}}$ should satisfy the following constraints:

$$D_{\min} \le D_{k,m}^{\text{opt}} \le D_{\max}. \tag{39}$$

Finally, to ensure the safety of train operations, the maximum tracking speed between adjacent trains should be less than the critical value v_{limit}. Based on the kinematics formula, we know that $v_2^2 - v_1^2 = 2as$, v_2 is the terminal velocity, v_1 is the initial velocity, a is the acceleration, and s is the distance. Therefore, the speed v_{kij} should be expressed as $v_{kij} \le \sqrt{2L_{\text{limit}}a_{\text{dec}}^{\max}}$ to ensure that there is no conflict between the adjacent trains.

$$v_{kij} \le v_{\text{limit}} = \sqrt{2L_{\text{limit}}a_{\text{dec}}^{\max}}. \tag{40}$$

3. Solution Method

The NSGA-II is a mature, multi-objective, intelligent optimization algorithm. It was first proposed by Deb et al. [32] to analyze and solve optimization problems of maximization or minimization. Furthermore, multi-objective optimization algorithms, such as NSGA, PAES, SPEA, MOEA/D, and NSGA-II, are very well-developed. A comparative analysis of the above algorithms is shown in Table 6.

Considering that the multi-objective optimization model established in this study does not belong to the high-dimensional optimization model after simplification, we apply the NSGA-II algorithm. The NSGA-II is a multi-objective programming algorithm with an elite strategy, which is better than the NSGA algorithm. Compared with the NSGA algorithm, it can reduce the complexity of the model and get the optimization results faster. Furthermore, the NSGA-II algorithm has been effectively applied in the field of transportation in the past (Jemai et al. [33]). Finally, considering that the scale of the actual case studied in this study is not very large, the NSGA-II algorithm can be used to solve the problem. The detailed description of the NSGA-II algorithm is given in Li et al. [31].

In summary, the basic steps of the NSGA-II algorithm are as follows, and the framework of the proposed NSGA-II algorithm is shown in Figure 7.

Step 1. The paternal generation, P_t, with population size N is randomly generated, and then the paternal generation population produces the same size offspring population, Q_t. The two populations are mixed to form a new population R_t with population size $2N$.

Step 2. Fast nondominant sequencing of new populations R_t is performed. At the same time, the crowding degree of all individuals in each nondominant layer is calculated. According to the nondominant relationship between individuals and the size of the individual crowding degree, the appropriate individuals should be selected to form a new parent population, P_{t+1}.

Step 3. Through the basic operation of the traditional genetic algorithm (crossover, mutation, and so on), a new offspring population Q_{t+1} is generated. When Q_{t+1} and P_{t+1} are mixed, a new population R_{t+1} is generated. The above operation is repeated until the condition of the end of the optimization problem is satisfied.

4. Numerical Experiments

4.1. Numerical Experiment Set-Up. Numerical experiments were conducted to verify the effectiveness of the proposed optimization model in the urban rail transit system based on the Yizhuang line in Beijing, China. Table 7 provides the input data for the Yizhuang line in Beijing, including section length, dwelling time, traveling time in the upward direction, and traveling time in the downward direction. The speed limit of trains for each section is 80 km/h. Considering passenger traveling comfort, the maximum acceleration of the train is 1 m/s^2, and the maximum deceleration of the train is −0.5 m/s^2, the headway between following trains during the nonpeak hours is 210 s. Other parameters are listed in Table 5.

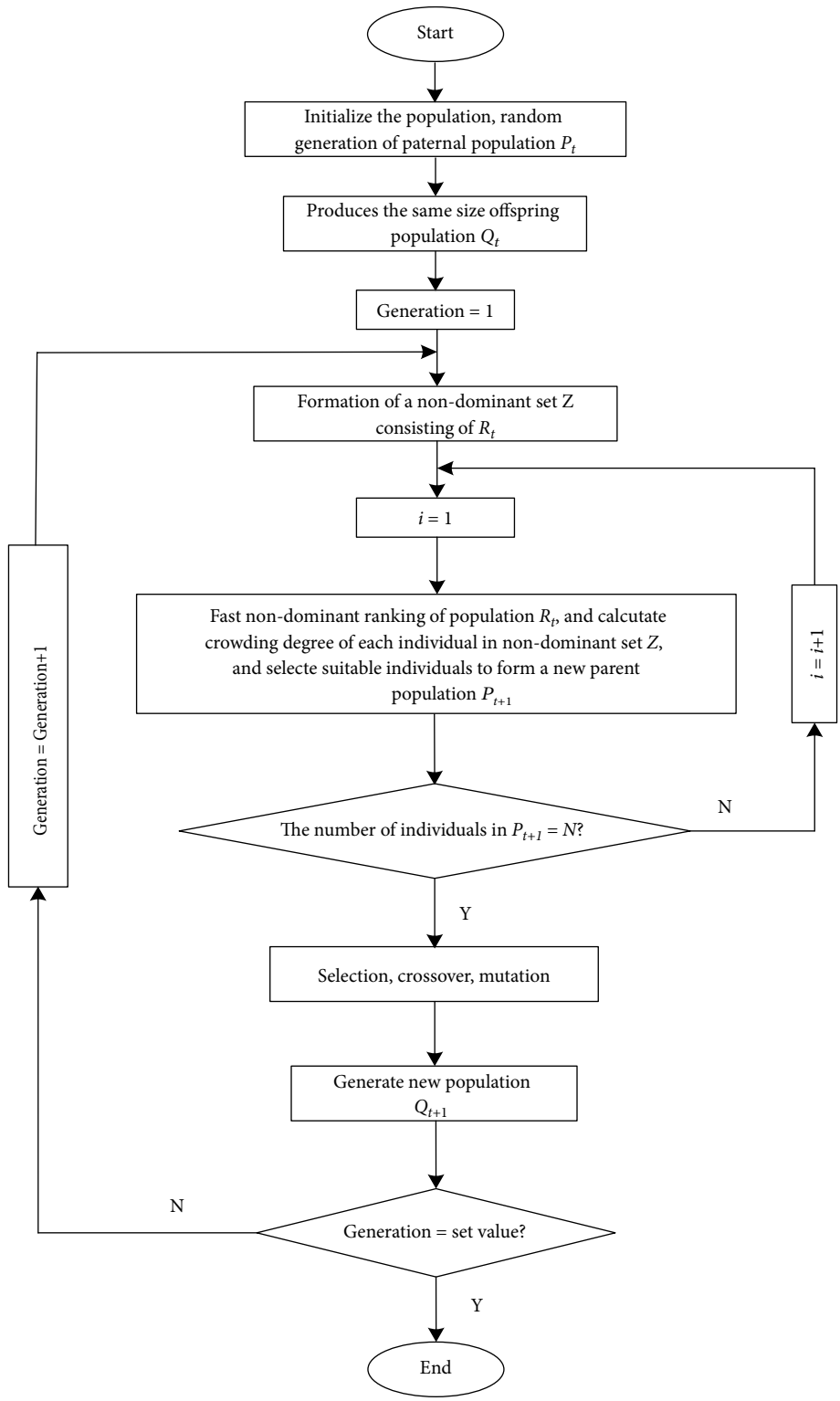

Figure 7: The framework of the NSGA-II algorithm.

4.2. Optimization Results Obtained by the NSGA-II Algorithm. We used a computer (CPU: Inter (R) Core (TM) i5-6100@3.7 GHz; 8 GB memory) to solve the proposed optimization problems. Specifically, we used the MATLAB software to solve our multi-objective programming model with the NSGA-II algorithm. For this case, our parameters are tuned as follows: the optimal individual coefficient = 0.3, population size = 100, generations = 200, the generation of stopping iteration = 200, and the error of fitness function = 1e-100. The solving time was less than one minute. Figures 8 and 9 present the Pareto solutions of the multi-objective programming model obtained by the NSGA-II algorithm.

Table 7: Input data of Yizhuang line in Beijing.

Station ID	M_1	M_2	M_3	M_4	M_5	M_6	M_7
Dwell time	40	40	40	40	40	40	40
Section length	2631	1275	2366	1982	993	1538	1280
Up direction	194	102	153	132	84	112	99
Down direction	195	105	157	135	90	111	101
Station ID	M_8	M_9	M_{10}	M_{11}	M_{12}	M_{13}	Total
Dwell time	40	40	40	40	40	40	520
Section length	1354	2338	2265	2086	1286		21394
Up direction	102	158	146	137	99		1518
Down direction	103	162	150	141	100		1550

Note: "Up direction" represents traveling time in the up direction (M_1 -> M_{13}); "Down direction" represents traveling time in the down direction (M_{13} -> M_1).

Table 8: The optimized running time of three phases in each section.

Up direction	Accelerating time/s	Coasting time/s	Braking time/s	Down direction	Accelerating time/s	Coasting time/s	Braking time/s
M_1-M_2	16.43	161.06	16.51	M_{13}-M_{12}	16.24	65.09	18.67
M_2-M_3	15.65	68.50	17.85	M_{12}-M_{11}	18.15	102.73	20.12
M_3-M_4	18.91	113.28	20.81	M_{11}-M_{10}	18.46	111.24	20.30
M_4-M_5	18.60	92.47	20.93	M_{10}-M_9	17.51	125.74	18.75
M_5-M_6	15.23	51.01	17.76	M_9-M_8	16.58	67.38	19.04
M_6-M_7	17.19	75.20	19.61	M_8-M_7	15.93	66.83	18.24
M_7-M_8	16.38	63.74	18.88	M_7-M_6	17.40	73.69	19.91
M_8-M_9	16.80	65.84	19.36	M_6-M_5	13.81	60.43	15.76
M_9-M_{10}	18.00	120.51	19.49	M_5-M_4	18.08	96.74	20.18
M_{10}-M_{11}	19.06	105.76	21.18	M_4-M_3	18.36	118.66	19.98
M_{11}-M_{12}	18.80	97.13	21.07	M_3-M_2	15.07	72.92	17.01
M_{12}-M_{13}	16.47	63.53	19.00	M_2-M_1	16.35	162.27	16.38

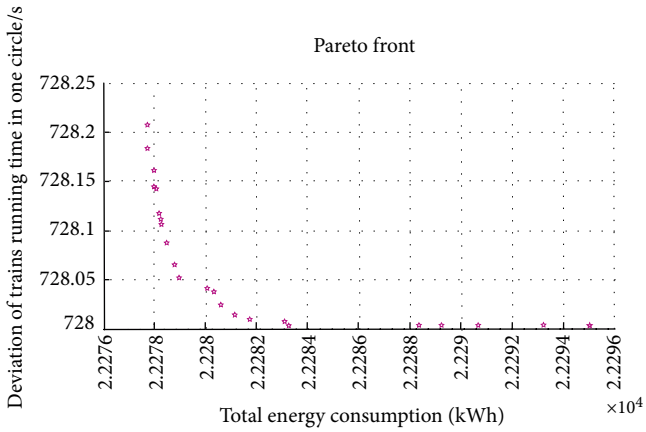

Figure 8: The Pareto solutions of OEST.

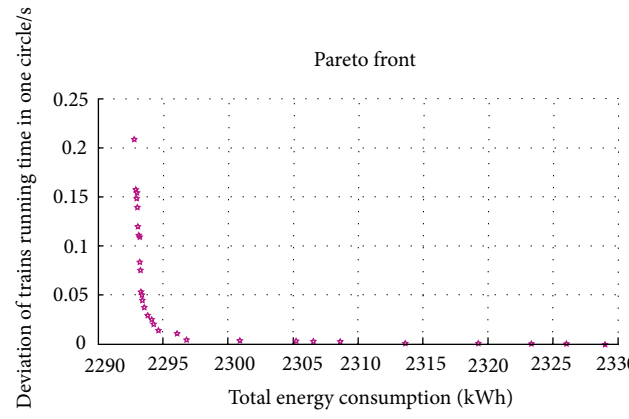

Figure 9: The Pareto solutions of OQOST.

They give 30 good solutions with different weight ratios, respectively. Among them, Figure 8 shows 30 good solutions of the objective function in the case of $\lambda_e/\lambda_s = 10:1$ and the optimal solution is $E_{\text{total}} = 2228.55$ kWh and $\varepsilon_{\text{total}} = 728$ s. This is the optimal result of the optimal energy-saving timetable (OEST). Figure 9 shows 30 good solutions of the objective function in the case of $\lambda_e/\lambda_s = 1:10$ and the optimal solution is $E_{\text{total}} = 2292.81$ kWh and $\varepsilon_{\text{total}} = 0$ s. This is the optimal result of the optimal quality of service timetable (OQOST). In addition, the optimized running time for the three phases in each section and the solution results of decision variables, which leads to the optimized dwell time, are provided in Tables 8 and 9.

4.3. Comprehensive Analysis of the Optimized Results. Figure 10 shows the regenerative braking energy utilization ratio in each section of the current timetable. Figure 11 shows the

Table 9: The optimized dwell time of optimized timetable.

Up direction	Optimized dwell time/s		Down direction	Optimized dwell time/s	
	OEST	OQOST		OEST	OQOST
M_1	40	40	M_{13}	40	40
M_2	45	45	M_{12}	30	30
M_3	45	45	M_{11}	21	21
M_4	29	35	M_{10}	40	45
M_5	30	45	M_9	45	45
M_6	36	36	M_8	45	45
M_7	45	45	M_7	45	45
M_8	45	45	M_6	37	37
M_9	45	45	M_5	30	37
M_{10}	40	45	M_4	27	45
M_{11}	24	24	M_3	45	45
M_{12}	30	30	M_2	45	45
M_{13}	40	40	M_1	40	40
Total time/s	494	520	Total time/s	490	520

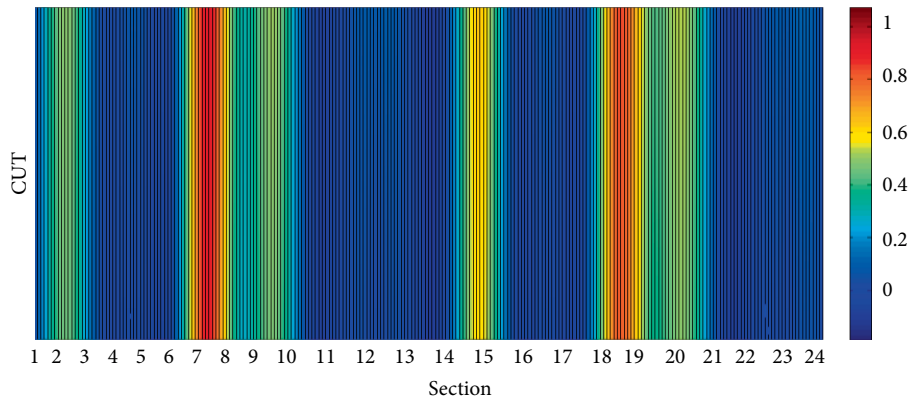

Figure 10: The regenerative braking energy utilization ratio in each section of the CUT.

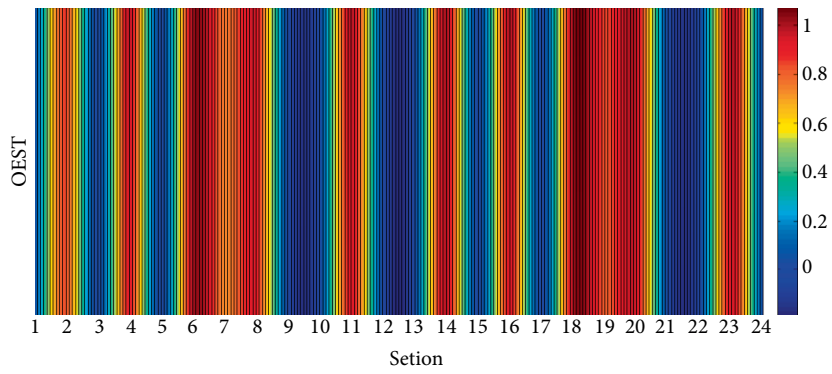

Figure 11: The regenerative braking energy utilization ratio in each section of the OEST.

regenerative braking energy utilization ratio in each section of the OEST. Figure 12 shows the regenerative braking energy utilization ratio in each section of the OQOST. We conclude that the energy utilization ratio of regenerative braking in sections of optimized timetables is significantly improved. The highest average regenerative braking energy utilization rate is provided by the OEST solution. The CUT has the lowest, and the OQOST is between the two.

Table 10 presents a comparison of energy saving and the quality of service between the current timetable (CUT) and optimized timetables (OEST and OQOST). The total energy consumption of the current timetable was 2441.53 kW, and the

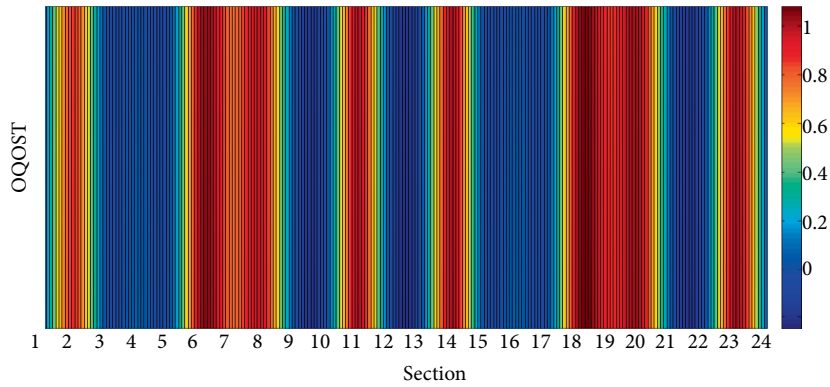

Figure 12: The regenerative braking energy utilization ratio in each section of the OQOST.

Table 10: Comparison of energy saving and quality of service between the current timetable and optimized timetables.

	Current timetable		Optimized timetables			
			OEST		OQOST	
Direction	Up	Down	Up	Down	Up	Down
Overlapping time/s	492.05	502.71	1380.08	1401.14	1114.88	1140.36
Available regenerative braking energy/(kWh)	53.95	52.78	161.72	157.95	128.24	126.26
Average regenerative braking utilization ratio	0.18	0.19	0.46	0.49	0.38	0.40
Total energy consumption/(kWh)	2441.53		2228.55		2292.81	
The deviation of trains running time in one circle/s	0		728		0	

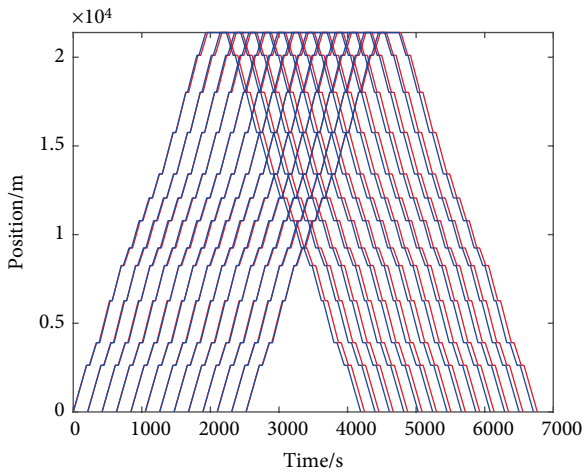

Figure 13: A comparison of the CUT (red lines) and the OEST (blue lines).

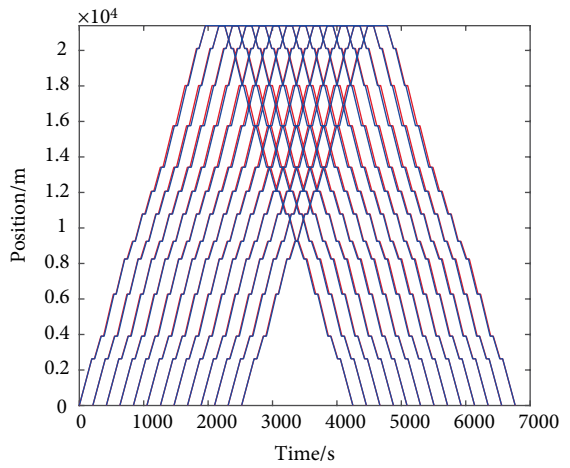

Figure 14: A comparison of the CUT (red lines) and the OQOST (blue lines).

deviation of trains running time in one circle was 0 s. The total energy consumption of OEST was 2228.55 kWh, and the deviation of trains running time in one circle was 728 s, thus indicating energy savings of up to 8.72%. Nonetheless, the deviation of train running time in one circle of 728 s, impacts the quality of service negatively. The total energy consumption was 2292.81 kWh, and the deviation of train running time in one circle was 0 s in OQOST. This indicates energy savings of up to 6.09%, without increasing the deviation of train running time.

4.4. Comprehensive Analysis of the Optimized Timetables. We compared the CUT and the optimized timetables (OEST and OQOST). Figures 13 and 14 present the timetabling of the urban rail transit system under the CUT and under the optimized timetables (OEST and OQOST). Figure 13 shows a comparison of the CUT and the OEST. Table 11 gives the optimized timetable for the first train of the OEST. We identified the deviation of train running time in one circle between the timetables of 56 s. Figure 14 presents a comparison of the CUT and the OQOST. Table 12 gives the optimized timetable for the first train of the OQOST. We identified the deviation of train running time in one circle between the timetables of 0 s. Therefore, we conclude that if the decision-makers are more concerned about energy saving than the quality of services,

Table 11: The optimized timetable for the first train of the OEST.

Up	M1	M2	M3	M4	M5	M6	M7
Dwell (s)	—	45	45	29	30	36	45
Arrival (s)	—	194	341	539	700	814	962
Departure (s)	0	239	386	568	730	850	1007
Up	M8	M9	M10	M11	M12	M13	—
Dwell (s)	45	45	40	24	30	—	—
Arrival (s)	1106	1253	1456	1642	1803	1932	—
Departure (s)	1151	1298	1496	1666	1833	—	—
Down	M13	M12	M11	M10	M9	M8	M7
Dwell (s)	—	30	21	40	45	45	45
Arrival (s)	—	2332	2503	2674	2876	3024	3170
Departure (s)	2232	2362	2524	2714	2921	3069	3215
Down	M6	M5	M4	M3	M2	M1	—
Dwell (s)	37	30	27	45	45	—	—
Arrival (s)	3326	3453	3618	3802	3952	4192	—
Departure (s)	3363	3483	3645	3847	3997	—	—

Table 12: The optimized timetable for the first train of the OQOST.

Up	M1	M2	M3	M4	M5	M6	M7
Dwell (s)	—	45	45	35	45	36	45
Arrival (s)	—	194	341	539	706	835	983
Departure (s)	0	239	386	574	751	871	1028
Up	M8	M9	M10	M11	M12	M13	—
Dwell (s)	45	45	45	24	30	—	—
Arrival (s)	1127	1274	1477	1668	1829	1958	—
Departure (s)	1172	1319	1522	1692	1859	—	—
Down	M13	M12	M11	M10	M9	M8	M7
Dwell (s)	—	30	21	45	45	45	45
Arrival (s)	—	2358	2529	2700	2907	3055	3201
Departure (s)	2258	2388	2550	2745	2952	3100	3246
Down	M6	M5	M4	M3	M2	M1	—
Dwell (s)	37	37	45	45	45	—	—
Arrival (s)	3357	3484	3656	3858	4008	4248	—
Departure (s)	3394	3521	3701	3903	4053	—	—

the OEST is better than the OQOST. On the contrary, if the decision-makers prioritize the quality of services above energy saving, the OQOST is better than the OEST.

4.5. Main Parametric Analysis of the Algorithm. To verify the robustness of results, we analyze the main parameters, Generations (G) and the Optimal Individual Coefficient (OIC), of the algorithm. By changing the values of parameters G and OIC, we get Pareto solutions of OEST and OQOST under different parameters, as shown in Figures 15–23. In addition, we compare and analyze all E_{total} and ε_{total} of the different optimization timetables under different parameters, as shown in Table 13. From Table 13, we get the following results: when G is unchanged, E_{total} increases slightly with an increase of OIC, while ε_{total} basically does not change. When OIC is unchanged, E_{total} decreases slightly with an increase of G, while ε_{total} basically does not change. We infer that the algorithm has some randomness, but these slight changes do not affect the effectiveness of the algorithm.

4.6. Sensitivity Analysis of the Main Parameters. With the continuous progress and development of science and technology and the growing advocacy for green transportation, graphene is expected to be used in urban rail transit systems in the future. Graphene's most useful characteristic, in this regard, is that its resistivity is almost zero (Ferrari et al. [34]). It is thus a perfect conductive material. If graphene could be used in the power supply systems of urban rail transit systems, it would greatly reduce the transmission and consumption of electric energy. In terms of the variable of this study, it would greatly improve ξ. Therefore, we conducted a sensitivity analysis for the regenerative braking energy conversion rate, ξ. To this end, it is assumed that the sensitivity range of ξ is 0.7–1.0 and that the step length is 0.05. In addition, the m_{totol} given in Table 5

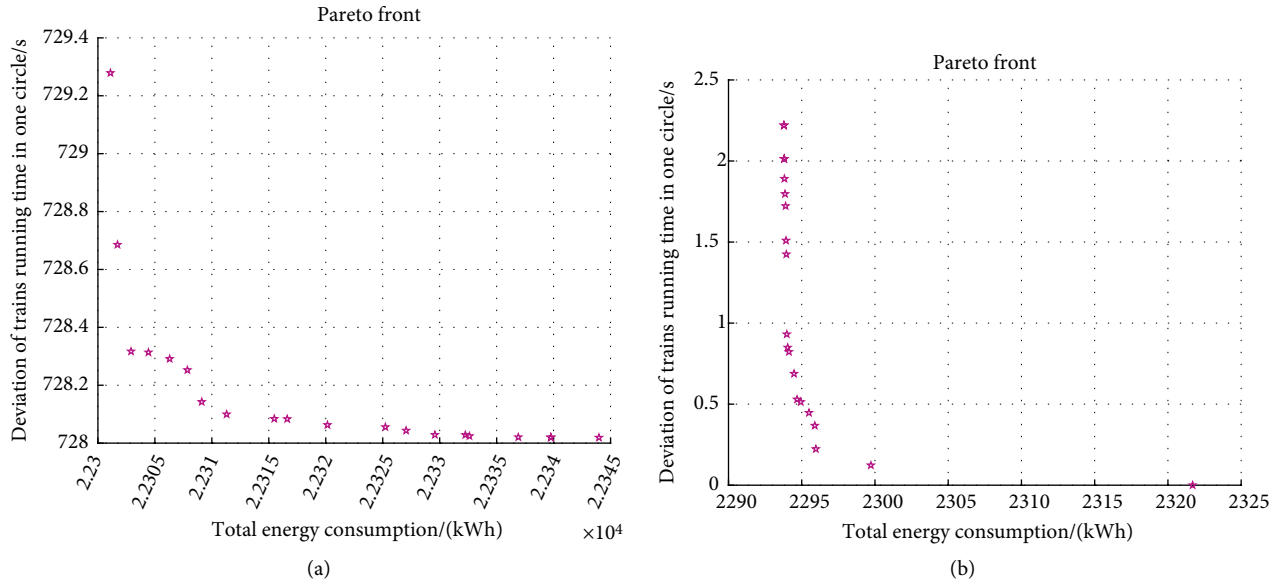

FIGURE 15: The Pareto front under $G = 150$ and OIC = 0.2. (a) The Pareto solutions of the OEST. (b) The Pareto solutions of the OQOST.

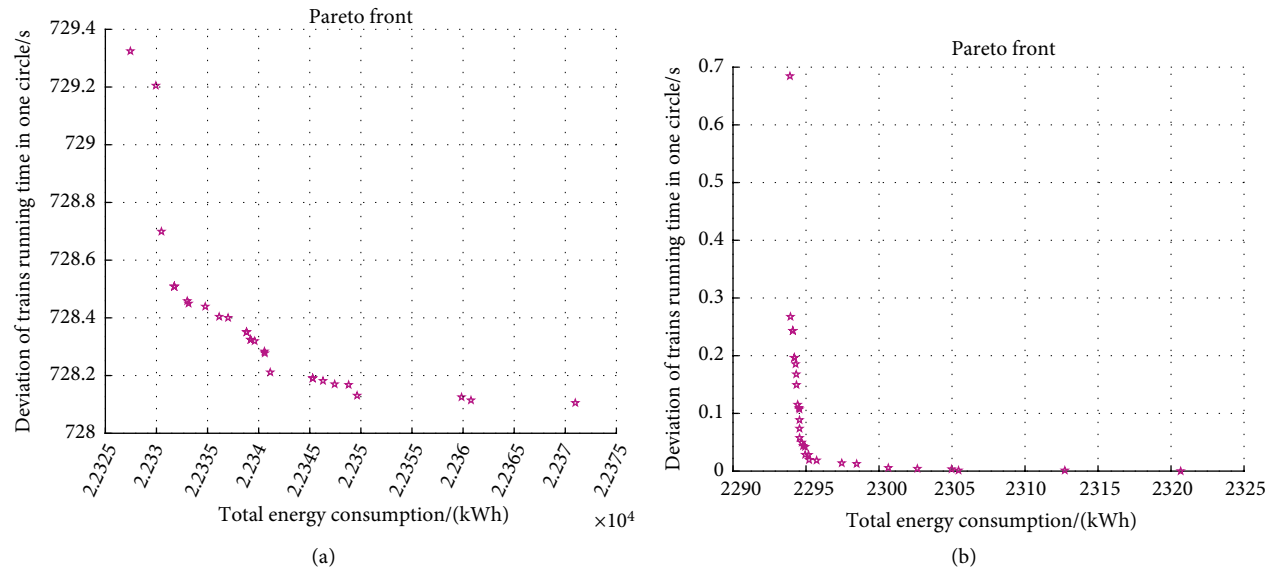

FIGURE 16 : The Pareto front under $G = 150$ and OIC = 0.3. (a) The Pareto solutions of the OEST. (b) The Pareto solutions of the OQOST.

is only the total weight of an empty train, but the actual weight of a train consists of the weight of an empty train and the total weight of the passengers on the train. According to the data in Yin et al. [23], the total weight of a train at full load is 282375 kg, so we assume that the sensitivity range of m_{totol} is 194295 kg–284295 kg and that the step length is 10000 kg. We obtained a trade-off between the main parameters and E_{total}, as shown in Figure 24. Figure 24 considers three timetables: CUT, OEST, and OQOST. The horizontal axis represents the total weight of the train, the vertical axis represents the regenerative braking energy conversion rate, and the color depth in the figure represents the total energy consumption of all trains. We can see that, with the increase of ξ, the total energy consumption of the operation decreases significantly. With the increase of train weight, the total energy consumption of the operation increases significantly.

5. Conclusions

This study focused on developing an optimal train energy-saving strategy and timetable optimization method to improve the overlapping time between following trains and thus, increase the utilization of regenerative braking energy. Considering that timetable changes may affect the quality of the transport service, we proposed a multi-objective optimization model for urban railways, which is designed to minimize the total energy consumption of trains, while maximizing

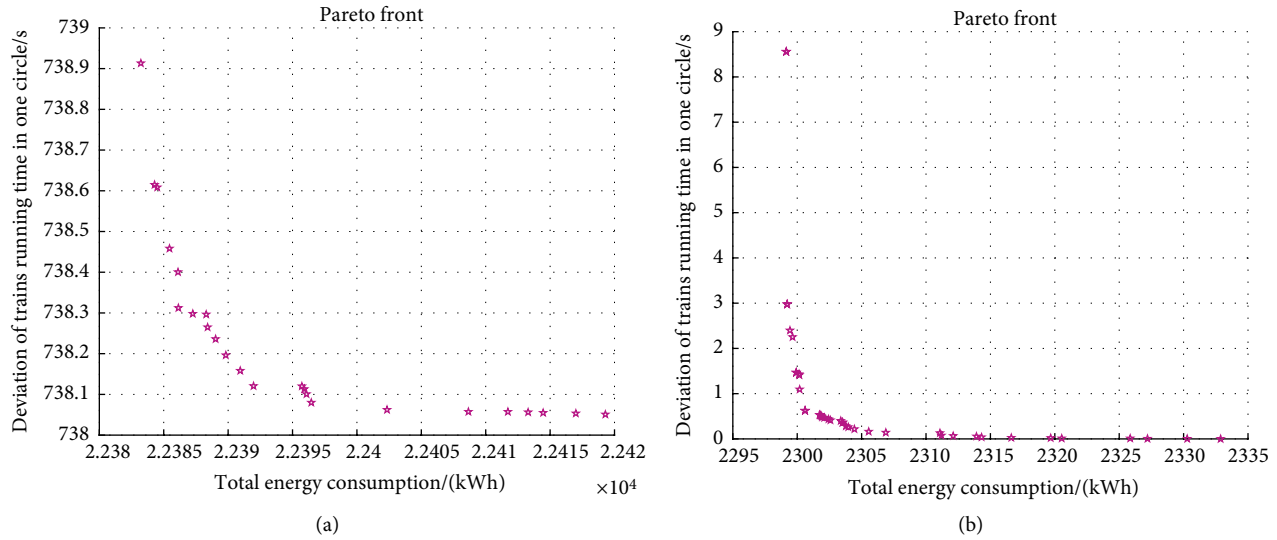

Figure 17: The Pareto front under $G = 150$ and OIC = 0.4. (a) The Pareto solutions of the OEST. (b) The Pareto solutions of the OQOST.

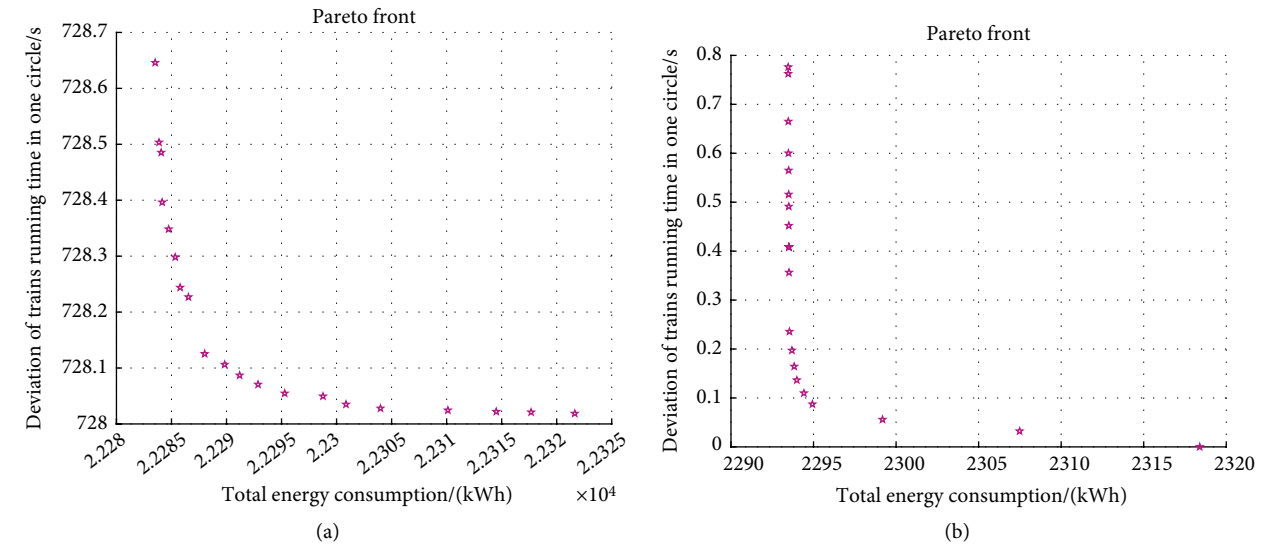

Figure 18: The Pareto front under $G = 200$ and OIC = 0.2. (a) The Pareto solutions of the OEST. (b) The Pareto solutions of the OQOST.

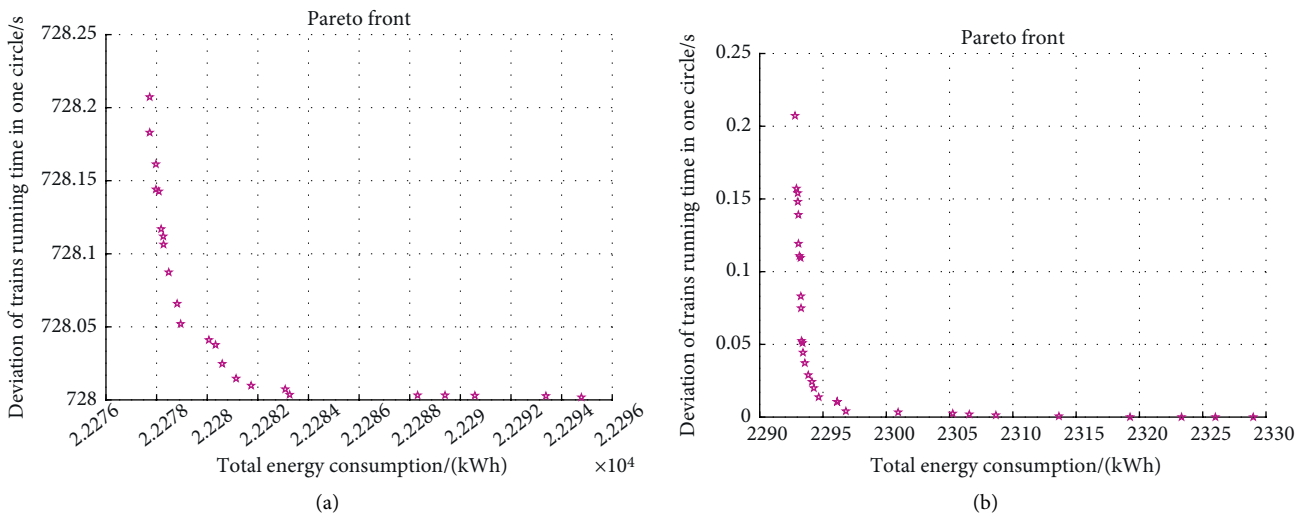

Figure 19: The Pareto front under $G = 200$ and OIC = 0.3. (a) The Pareto solutions of the OEST. (b) The Pareto solutions of the OQOST.

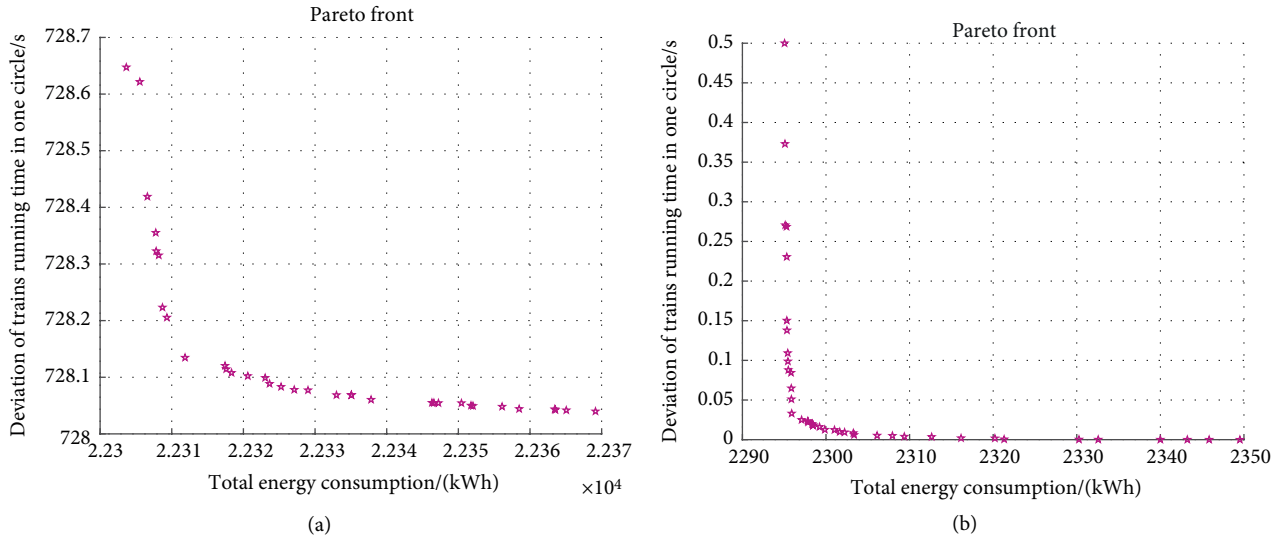

Figure 20: The Pareto front under $G = 200$ and OIC = 0.4. (a) The Pareto solutions of the OEST. (*b*) The Pareto solutions of the OQOST.

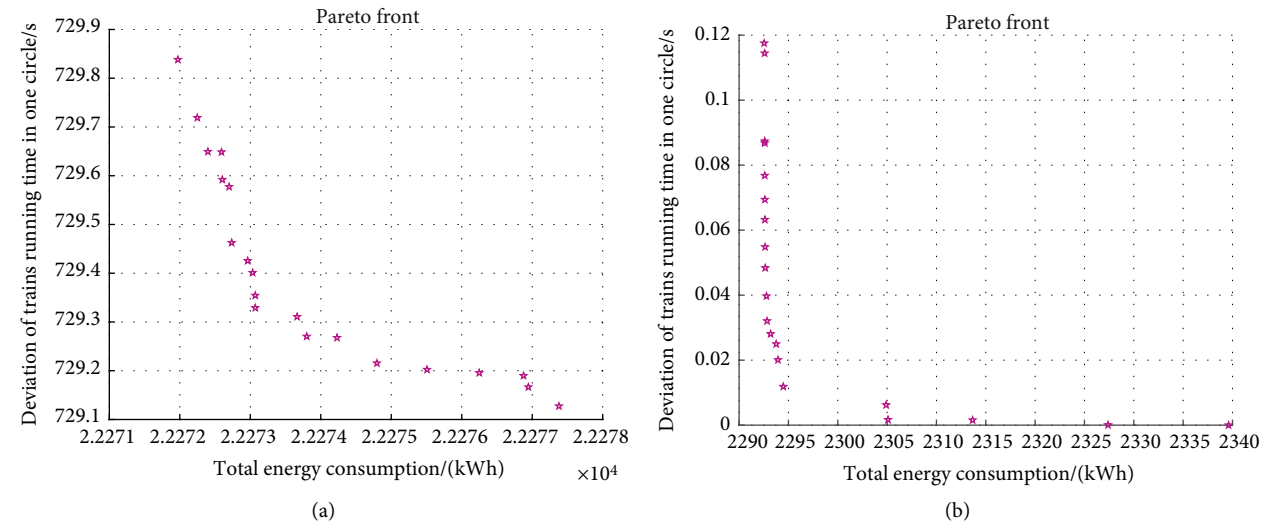

Figure 21: The Pareto front under $G = 250$ and OIC = 0.2. (a) The Pareto solutions of the OEST. (b) The Pareto solutions of the OQOST.

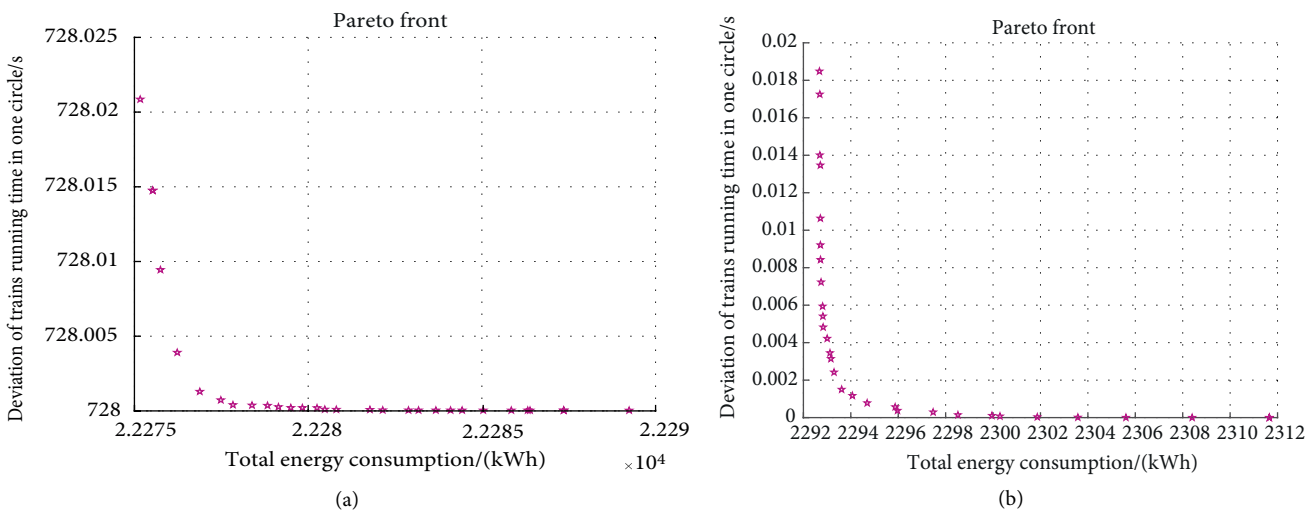

Figure 22: The Pareto front under $G = 250$ and OIC = 0.3. (a) The Pareto solutions of the OEST. (b) The Pareto solutions of the OQOST.

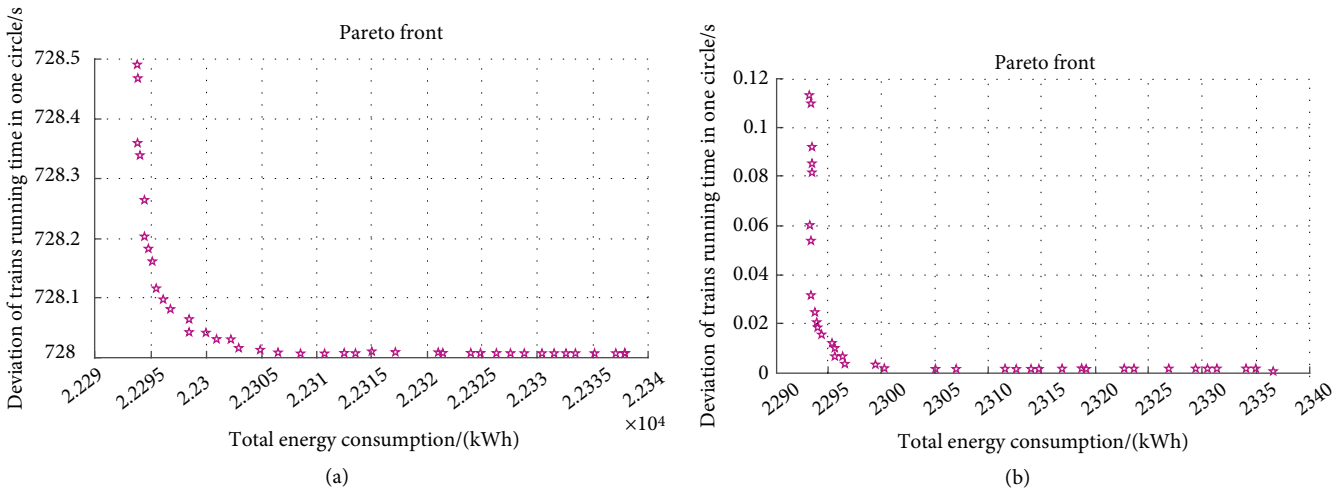

FIGURE 23: The Pareto front under $G = 250$ and OIC = 0.4. (a) The Pareto solutions of the OEST. (b) The Pareto solutions of the OQOST.

TABLE 13: The values of OEST and OQOST with different main parameters of the algorithm.

Generations (G)	Optimal individual coefficient (OIC)	OEST		OQOST	
		E_{total}/kWh	ε_{total}/s	E_{total}/kWh	ε_{total}/s
150	0.2	2230.10	728	2293.80	0
	0.3	2233.05	728	2294.11	0
	0.4	2238.30	738	2296.13	0
200	0.2	2228.40	728	2292.67	0
	0.3	2228.55	728	2292.81	0
	0.4	2230.42	728	2295.01	0
250	0.2	2227.21	729	2292.50	0
	0.3	2227.52	728	2292.71	0
	0.4	2229.46	728	2293.12	0

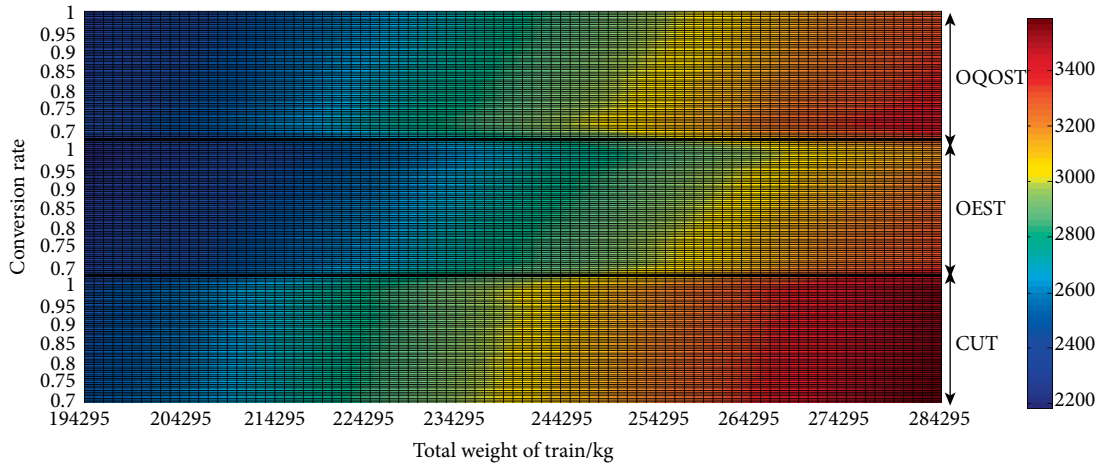

FIGURE 24: A comparison between the main parameters and total energy consumption under different timetables.

the quality of service. Furthermore, considering the conflicting requirements of decision-makers, we added weight factors to the objective functions to reflect decision-makers' preferences for energy-saving and the quality of services. During the model solving process, the NSGA-II algorithm was selected as an effective method to obtain optimal solutions. Finally, a practical case study was selected to verify the effectiveness of the proposed model, as well as to evaluate the advantages of the OEST and the OQOST. In the future, the proposed model may be solved by more advanced algorithms or simulation methods. In order to satisfy the requirements of the real-world, future research should strengthen the proposed model so that

it will be able to integrate timetabling optimization, energy-saving ramp planning, and other practical constraints.

Data Availability

The data are available by contacting wenchao@swjtu.cn.

Conflicts of Interest

The authors declare that they have no conflicts of interest.

Acknowledgments

This work was supported by the National Key R&D Program [grant number 2017YFB1200700], The National Natural Science Foundation of China [grant number U1834209 and 71871188]. We acknowledge the support of the State Key Laboratory of Rail Traffic Control [grant number RCS2019K007] and the China Scholarship Council. We are grateful for the useful contributions made by our project partners.

References

[1] Q. Gu, T. Tang, F. Cao, and Y.-D. Song, "Energy-efficient train operation in urban rail transit using real-time traffic information," *IEEE Transactions on Intelligent Transportation Systems*, vol. 15, no. 3, pp. 1216–1233, 2014.

[2] P. Howlett, I. Milroy, and P. Pudney, "Energy-efficient train control," *Control Engineering Practice*, vol. 2, no. 2, pp. 193–200, 1994.

[3] R. R. Liu and I. M. Golovitcher, "Energy-efficient operation of rail vehicles," *Transportation Research Part A: Policy and Practice*, vol. 37, no. 10, pp. 917–932, 2003.

[4] S. Su, T. Tang, L. Chen, and B. Liu, "Energy-efficient train control in urban rail transit systems," *Proceedings of the Institution of Mechanical Engineers, Part F: Journal of Rail and Rapid Transit*, vol. 229, no. 4, pp. 446–454, 2015.

[5] E. Khmelnitsky, "On an optimal control problem of train operation," *IEEE Transactions on Automatic Control*, vol. 45, no. 7, pp. 1257–1266, 2000.

[6] M. Peña-Alcaraz, A. Fernández, A. P. Cucala, A. Ramos, and R. R. Pecharromán, "Optimal underground timetable design based on power flow for maximizing the use of regenerative-braking energy," *Proceedings of the Institution of Mechanical Engineers, Part F: Journal of Rail and Rapid Transit*, vol. 226, no. 4, pp. 397–408, 2012.

[7] X. Yang, X. Li, Z. Gao, H. Wang, and T. Tang, "A cooperative scheduling model for timetable optimization in subway systems," *IEEE Transactions on Intelligent Transportation Systems*, vol. 14, no. 1, pp. 438–447, 2013.

[8] X. Li and H. K. Lo, "An energy-efficient scheduling and speed control approach for metro rail operations," *Transportation Research Part B: Methodological*, vol. 64, pp. 73–89, 2014.

[9] A. Higgins, E. Kozan, and L. Ferreira, "Optimal scheduling of trains on a single line track," *Transportation Research Part B: Methodological*, vol. 30, no. 2, pp. 147–161, 1996.

[10] L. Yang, K. Li, and Z. Gao, "Train timetable problem on a single-line railway with fuzzy passenger demand," *IEEE Transactions on Fuzzy Systems*, vol. 17, no. 3, pp. 617–629, 2009.

[11] P. Howlett, "Optimal strategies for the control of a train," *Automatica*, vol. 32, no. 4, pp. 519–532, 1996.

[12] A. Ramos, M. T. Pena, A. Fernández, and P. Cucala, "Mathematical programming approach to underground timetabling problem for maximizing time synchronization," *Management and Organization*, vol. 35, pp. 88–95, 2008.

[13] D. Fournier, D. Mulard, and F. Fages, "Energy optimization of metro timetables: a hybrid approach," in *The 18th International Conference on Principles and Practice of Constraint Programming*, pp. 7–12, Lecture Notes Computer Science, Springer, Berlin, 2012.

[14] A. Nasri, M. F. Moghadam, and H. Mokhtari, "Timetable optimization for maximum usage of regenerative energy of braking in electrical railway systems," in *SPEEDAM*, pp. 1218–1221, IEEE, Pisa, Italy, 2010.

[15] X. Li and X. Yang, "A stochastic timetable optimization model in subway systems," *International Journal of Uncertainty, Fuzziness and Knowledge-Based Systems*, vol. 21, 1pp. 1–15, 2013.

[16] H. Sun, J. Wu, H. Ma, X. Yang, and Z. Gao, "A bi-objective timetable optimization model for urban rail transit based on the time-dependent passenger volume," *IEEE Transactions on Intelligent Transportation Systems*, vol. 20, no. 2, pp. 604–615, 2019.

[17] Y. Bocharnikov, A. Tobias, and C. Roberts, "Reduction of train and net energy consumption using genetic algorithms for trajectory optimisation," in *IET Conference on Railway Traction Systems (RTS 2010)*, pp. 32–36, IEEE, Birmingham, UK, 2010.

[18] E. Rodrigo, S. Tapia, J. Mera, and M. Soler, "Optimizing electric rail energy consumption using the Lagrange multiplier technique," *Journal of Transportation Engineering*, vol. 139, no. 3, pp. 321–329, 2013.

[19] D. Tuyttens, H. Fei, M. Mezmaz, and J. Jalwan, "Simulation-based genetic algorithm towards an energy-efficient railway traffic control," *Mathematical Problems in Engineering*, vol. 2013, Article ID 805410, 12 pages, 2013.

[20] P. Wang and R. M. Goverde, "Multiple-phase train trajectory optimization with signalling and operational constraints," *Transportation Research Part C: Emerging Technologies*, vol. 69, pp. 255–275, 2016.

[21] X. Luan, Y. Wang, B. De Schutter, L. Meng, G. Lodewijks, and F. Corman, "Integration of real-time traffic management and train control for rail networks-part 2: extensions towards energy-efficient train operations," *Transportation Research Part B: Methodological*, vol. 115, pp. 72–94, 2018.

[22] K. Huang, J. Wu, X. Yang, Z. Gao, F. Liu, and Y. Zhu, "Discrete train speed profile optimization for urban rail transit: a data-driven model and integrated algorithms based on machine learning," *Journal of Advanced Transportation*, vol. 2019, Article ID 7258986, 17 pages, 2019.

[23] J. Yin, T. Tang, L. Yang, Z. Gao, and B. Ran, "Energy-efficient metro train rescheduling with uncertain time-variant passenger demands: an approximate dynamic programming approach," *Transportation Research Part B: Methodological*, vol. 91, pp. 178–210, 2016.

[24] G. M. Scheepmaker, R. M. Goverde, and L. G. Kroon, "Review of energy-efficient train control and timetabling," *European Journal of Operational Research*, vol. 257, no. 2, pp. 355–376, 2017.

[25] H. Ye and R. Liu, "Nonlinear programming methods based on closed-form expressions for optimal train control," *Transportation Research Part C: Emerging Technologies*, vol. 82, pp. 102–123, 2017.

[26] X. Yang, A. Chen, X. Li, B. Ning, and T. Tang, "An energy-efficient scheduling approach to improve the utilization of regenerative energy for metro systems," *Transportation Research Part C: Emerging Technologies*, vol. 57, pp. 13–29, 2015.

[27] M. Miyatake and H. Ko, "Optimization of train speed profile for minimum energy consumption," *IEEJ Transactions on Electrical and Electronic Engineering*, vol. 5, no. 3, pp. 263–269, 2010.

[28] X. Yang, A. Chen, J. Wu, Z. Gao, and T. Tang, "An energy-efficient rescheduling approach under delay perturbations for metro systems," *Transportmetrica B: Transport Dynamics*, vol. 7, no. 1, pp. 386–400, 2019.

[29] Z. Hou, H. Dong, S. Gao, G. Nicholson, L. Chen, and C. Roberts, "Energy-saving metro train timetable rescheduling model considering ATO profiles and dynamic passenger flow," *IEEE Transactions on Intelligent Transportation Systems*, vol. 20, no. 7, pp. 2774–2785, 2019.

[30] R. Chevrier, P. Pellegrini, and J. Rodriguez, "Energy saving in railway timetabling: A bi-objective evolutionary approach for computing alternative running times," *Transportation Research Part C: Emerging Technologies*, vol. 37, pp. 20–41, 2013.

[31] W. Li, Q. Peng, Q. Li, C. Wen, Y. Zhang, and J. Lessan, "Joint operating revenue and passenger travel cost optimization in urban rail transit," *Journal of Advanced Transportation*, vol. 2018, Article ID 7805168, 15 pages, 2018.

[32] K. Deb, A. Pratap, S. Agarwal, and T. Meyarivan, "A fast and elitist multiobjective genetic algorithm: NSGA-II," *IEEE Transactions on Evolutionary Computation*, vol. 6, no. 2, pp. 182–197, 2002.

[33] J. Jemai, M. Zekri, and K. Mellouli, "An NSGA-II algorithm for the green vehicle routing problem," *European Conference on Evolutionary Computation in Combinatorial Optimization*, Springer, Berlin, Heidelberg, pp. 37–48, 2012.

[34] A. Ferrari, J. Meyer, V. Scardaci et al., "Raman spectrum of graphene and graphene layers," *Physical Review Letters*, vol. 97, no. 18, Article ID 187401, 2006.